Scientific Research Publishing

International Journal of Geosciences, 2023, 14, 547-583
https://www.scirp.org/journal/ijg
ISSN Online: 2156-8367
ISSN Print: 2156-8359

Theory of the Origin of Terrestrial and Lunar Ores

Alexander N. Safronov

Obukhov Institute of Atmospheric Physics, Russian Academy of Sciences, Moscow, Russia
Email: safronov_2003@mail.ru

How to cite this paper: Safronov, A.N. (2023) Theory of the Origin of Terrestrial and Lunar Ores. *International Journal of Geosciences*, **14**, 547-583.
https://doi.org/10.4236/ijg.2023.146030

Received: May 7, 2023
Accepted: June 26, 2023
Published: June 29, 2023

Abstract

In this study, the theory of ore formation on the Earth and the Moon was developed. It is shown that ore deposits on the Earth and the Moon were mainly formed simultaneously with the separation of the Moon from the protoplanet and the formation of the oldest continents. The formation of terrestrial ores occurred as a result of the release of intermediate and heavy chemical elements from the deep layers of the protoplanet and the subsequent process of adhesion to old terrestrial geological faults. The time of terrestrial and lunar ores formations corresponds to the boundary between the Tonian and Cryogenian Periods (~720 Ma). Lunar ore formation processes are different on the near and far sides. The farside of the Moon is a single piece of the protoplanetary lithosphere, so ores there could be formed mainly due to the overflow of igneous rocks over the edge of the lunar continent. On the nearside, due to the rapid cooling, ores were formed in the area of navel-string during the drip-liquid separation of the Moon from the Earth. Due to the fact that the Moon separated at the first stage, the amount of water and methane on it is limited. In periods after the Cryogenian, volcanic, lava and sedimentary rocks on Earth could be enriched with intermediate elements due to the disruption of vertical stratification during galactic storms. To analyze this, a comparison of terrestrial volcanic and lunar pseudo-volcanic activity was carried out in the work.

Keywords

Comet Impact, Galaxy Storm, Galaxy Calm, Elemental Buoyancy Theory, Mantle-Core Layers, Ores Origin

1. Introduction

On March 11, 2011, the strongest Tohoku earthquake and tsunami occurred in

the Pacific Ocean about 72 km east of Honshu, Japan. The magnitude of this earthquake is estimated in the range of 9.0 - 9.1 (Mw). This natural disaster triggered a nuclear disaster at the Fukushima Daiichi Nuclear Power Plant of Tokyo Electric Power Company (TEPCO). After the 2011 disaster, the International Atomic Energy Agency (IAEA) began testing reactors, primarily industrial and scientific. However, this process was then extended to natural reactors. Recall that many years ago, in 1960, Kuroda first suggested the existence of a georeactor inside the earth [1]. Later Herndon and his colleagues investigated and developed this idea of the presence of a terrestrial reactor inside the Earth; see e.g. [2] [3] [4]. The Herndon terrestrial reactor was represented by a 12-kilometer layer in the center of the Earth.

However, Herndon's ideas were met with extreme aggression, which led to harsh criticism from Herndon [5]. As it is known, over the past 30 years, several groups of Herndon's opponents have been conducting experiments to register geoneutrinos and reconstructing the internal structure of the Earth. There are different schemes of such experiments; among them, there is also such scheme in which the recorded geoneutrinos were observed in the thickness of mountain ranges [6]-[12]. In recent years, there have been reports that ^{40}K and ^{235}U cannot be observed during such experiments, for example, see details in **Figure 1** in [13]. It turns out an amazing situation: for about 15 years, geoneutrino teams broke hard rocks, then for 10 years they installed equipment and collected statistics (10 - 20 events per year), then they held conferences, symposiums, published numerous articles in the highly rated journals, but after all the results of such prolonged and expensive experiments to determine the internal structure of the Earth completely unsatisfactory. The author and probably many readers are not interested in losing the image of these geoneutrino teams, as well as journals in which articles about geoneutrino research have been published. But the reaction of geoneutrino teams to criticism is interesting. In many journals, there is an opportunity to withdraw an article by the authors, or there are such sections as Comments or Notes, but we do not find any reaction to the censored remarks published by geoneutrino groups. The possibility of registering only fuel elements ^{232}Th and ^{238}U casts doubt on the feasibility of conducting lengthy and expensive experiments, such as the KamLAND and Borexino Experiments. Summing up the above, it is necessary to state that the attempt to restore the structure of the Earth by using geoneutrino experiments ended unsuccessfully even before the start of these experiments.

So, Hendon turned out to be an oracle that predicted the collapse of modern geophysics. A deep crisis struck planetary astrophysics in 2000-2010 (GIH, Giant Impact Hypothesis), geophysics in 2013 (geoneutrino experiments) and nuclear astrophysics in 2020-2022 (GCE, Galaxy Chemical Evolution) and continues to develop further in the form of a "*domino effect*". Thus, the process of degradation of science has spread to planetary astrophysics, which is a field of knowledge related to geophysics, and also studies the process occurring inside the

planet Earth.

By about 2000 - 2010, it was realized that there were no geochemical markers of the presence of the planet Thea, which casts doubt on the widely advertised version of the Giant Impact Hypothesis (GIH). Thus, the upcoming flights of Artemis (NASA), Luna-25 (RosCosmos) and Chang'e 6 (China National Space Administration, CNSA) will take place in the absence of a null hypothesis of the origin of the Moon. Any activities of an Aerospace Corporations that have invested billions of dollars in upcoming lunar missions and that are not provided with a scientific base are cause for concern.

Next, let's turn to the next "*domino*". Each star is a natural reactor, so after geophysics, it is time to test the validity of major principles of nuclear astrophysics. In 2020-2022, following geophysics and planetary astronomy, nuclear astrophysics failed the stress test. Since the verification process is currently ongoing, we will only briefly report on the presence of serious problems in the field of synthesis and transfer of chemical elements in the space of the Universe (GCE).

We have briefly outlined the situation and the crisis in science, now we will focus on the author's previous works and the place of this research in this series of authors' works. The relationship of this study with previous works is shown in **Figure 1**. This scheme demonstrates severe, moderate and minor impacts on the Earth, which were studied early in [14] [15] [16] [17]. In [14], the basic principles of creating habitable planets around stars in the Milky Way Galaxy were developed. In the work [15], the main goal is to study the causes of mass extinctions that occurred on Earth during galactic storms, and to create high-altitude stations to preserve the diversity of biological forms and lives. In [16] [17] the several tasks and goals were set at once, namely, at the first stage, the influence of planets on seismic and volcanic processes was studied, and a more fundamental task was set, which was to develop new principles in astrophysics that would allow the use of inertial interaction energy, significantly exceeding the energy of gravitational attraction, in order to easily overcome long distances between stars during interstellar missions.

The goal of this work is to study the origin of terrestrial and lunar ores. In the previous works of the author cited above, this issue was also considered, but due to the fact that they pursue other goals, insufficient attention was paid to the issue of the origin of ores. Please note that the ore formation process is not a one-step process. That is, we need to consider the terrestrial and lunar processes of ores origin as a three-stage process that occurred during a comet impact (**Figure 1(a)**), galaxy storms (**Figure 1(b)**), and galaxy calm (**Figure 1(c)**). We also announce the preparation for publication of a series of three papers on the study of the origin of life in the Milky Way Galaxy, [18] [19] [20]. In these works, we selected several stellar systems, located at a distance of ~200 pc from Earth, in which life and various biological forms could exist. These star systems were called DNA-stars. This cycle of works of [18] [19] [20] is represented in the

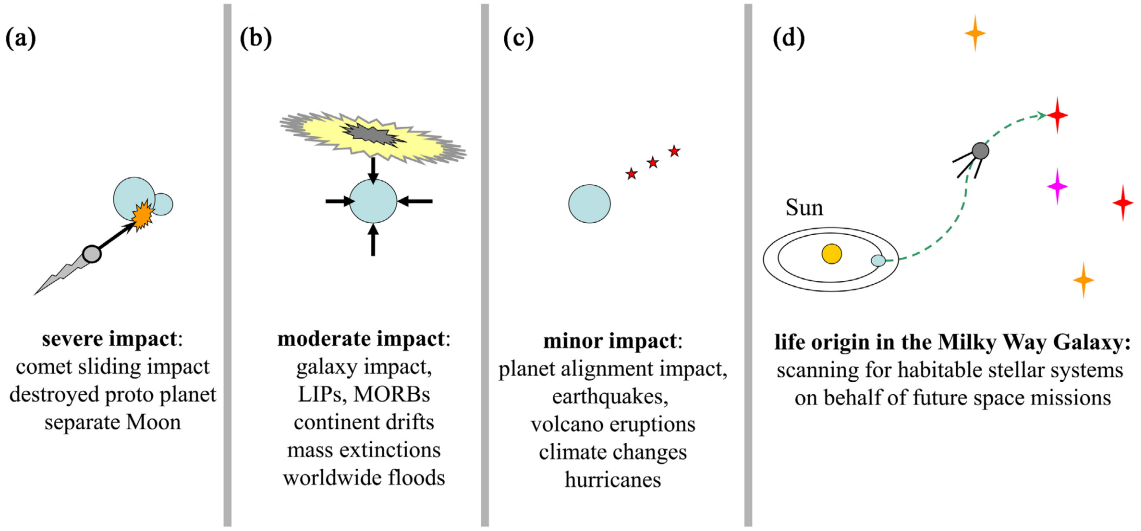

Figure 1. The scheme shows severe (a), moderate (b) and minor (c) impact to the Earth is presented as a three-stage process; (d) design of future interstellar mission.

scheme in Figure 1(d). It is absolutely obvious that at different stages of the evolution of the planet and their satellite, the processes of ore formation differ greatly both in the volume of ore formation and in their localization. This work is fundamental and may be of interest to geologists, geophysicists and astrophysicists.

2. Materials, Methods, and Hypotheses

2.1. The Lunar Datasets

In this study, we used the spatial distribution of some elements on the Moon, which were obtained by using the Lunar Prospector Gamma Ray Spectrometer (LPGRS) [21]. Recall that the different LPGRS abundances have different spatial resolution in the Global GIS Lunar Dataset [22]. In particular, the spatial resolution of calcium was equal to 5˚, the resolution of potassium, titanium, samarium, and silicon −2˚, and iron and thorium were −0.5˚ per pixel.

Lunar topography was presented by Kaguya topography (Araki *et al.*, 2009). The spatial distribution of lunar pyroclastic volcanic deposits and the locations of volcanic vents were obtained as a result of studies by Gaddis and colleges [23] [24].

To visualization the spatial distribution of these lunar elements, calculate the equator cross-sections, as well as the construction of lunar topography, the spatial distribution of lunar pyroclastic volcanic deposits and the location of volcanic vents, the full GIS-system ArcInfo system (Geo Information System, electronic cartography) was used and ESRI ArcInfo software [25] was applied.

2.2. Earth-Moon Hypotheses

There are several hypotheses of the formation of the Earth-Moon system. The most well-known hypotheses of the origin of the Earth-Moon are the fission

hypothesis, the evaporation hypothesis, the hypothesis of multiple moons, the hypothesis of joint formation from a protoplanetary dust disk, the capture hypothesis, the collision hypothesis, see, e.g. [26]. These studies were performed by three groups of scientists who used fundamentally different approaches to the problem of the origin of the Moon, namely astronomers and astrophysicists, geophysicists and geochemists, and more recently nuclear scientists. Each group of researchers has contributed to the development of the theory in accordance with the methods adopted in their field of knowledge. In the process of obtaining information about the Moon, one or another hypothesis dominated.

One of the first hypotheses is the fission hypothesis proposed in 1879 by G.H. Darwin [27]. According to this hypothesis, the Moon was formed as a result of the resonant effects of solar tides and centrifugal forces during a rapid rotation of the Earth around its axis. Later Ringwood and Wise updated Darwin's hypothesis to include models of thermal evolution, and in particular the fact that the Earth-Moon formation is preceded by a very high angular momentum of the proto-Earth, e.g. [28] [29]. The occurrence of large angular momentum at the Proto-Earth is impossible to explain, just as it is difficult to explain its sudden disappearance in modern Earth time. The hypothesis of co-formation from a protoplanetary dust disk was popular in the 1960-80s; e.g. [30] [31] and references in them.

Since the density of the Moon is less than the density of the Earth, independently and in parallel with the hypothesis of accretion from a dust disk, a capture hypothesis was developed in the 1960s, according to which the Earth captured the Moon. However, according to the capture hypothesis, the Proto-Earth must have a large initial atmosphere that would slow down the Moon's movement by natural aerobraking before it could escape. The capture hypothesis was extended to the Apollo and Luna missions.

In the post Apollo period, the giant-impact hypothesis (GIH) became a favored scientific hypothesis of the Earth-Moon formation, see, e.g. Benz and Cameron studies [32] [33] [34] [35] [36]. According to the GIH hypothesis, the Proto-Earth was collapsed with the planet, which is called as a Thea. We also remark a series of Canup and colleges works which was also devoted to investigate a various aspects of formation of the Earth-Moon system [37] [38] [39] [40].

Due to GIH collision, only the kinetic energy of the gravitational interaction was taken into account; therefore, in this hypothesis, it was necessary to assume that the hypothetical planet Thea had dimensions comparable to or exceeding the size of Mars. The GIH hypothesis explained many factors: the coincidence of the chemical composition of the Moon and the Earth; the Moon has a lower density than the Earth; the rotation of the Earth and the orbit of the Moon have a similar orientation; the fact that the surface of the Moon was once molten; the Moon has a relatively small iron core.

However, the euphoria quickly passed, as measurements of oxygen [41] [42] manganese and chromium [43] [44], titanium [45] [46], silicon [47] [48] and

other types of isotopes indicated that the Moon and the Earth have a very high degree of similarity. Therefore it was not possible to find any geochemical markers indicating the presence of such a massive body as Thea, so the GIH was declined.

Also, the GIH hypothesis required the formation of the Moon from a massive ocean of molten magma spilled from the bowels of the Proto-Earth, but the topography of the Moon is bimodal, and the shape of the Moon is far from an ellipsoid of rotation. The chemical composition of the near and far sides is very different, which is not consistent with the formation of the Moon from a homogeneous magmatic mass.

Since no geomarkers of the existence of the Thea planet were found, to eliminate this disadvantage Voronin, Anisichkin, de Meijer and van Westrenen proposed replacing a collision with a planet with collision with a small body [49] [50]. A 100-kilometer asteroid was chosen as such a body, so this hypothesis was called the Asteroid Impact Hypothesis (AIH). Note that in these studies it was suggested that the energy needed to separate the Moon from the Proto-Earth could have been obtained from the nuclear energy of the protoplanet itself.

Recall that Herndon was a pioneer in the development of a terrestrial reactor; see e.g. [4]. The Herndon terrestrial reactor was represented by a 12-kilometer layer in the center of the Earth. Since Herndon and Hollenbach did not study the separation of the Moon from the Earth, we will not dwell too long on the details of the Herndon's central Earth reactor. Unlike the Herndon reactor, the Earth reactor in the AIH hypothesis was represented by a layer of uranium located on the core-mantle boundary inside the Proto-Earth. Thus, according to the AIH hypothesis, when an asteroid collided, a nuclear explosion occurred deep inside the Proto-Earth, at a depth of 2800 km.

Note that the AIH hypothesis was also not without flaws. The AIH hypothesis does not answer the following questions: Is there any evidence that uranium isotopes are present at the core-mantle boundary? Why didn't the heavy isotopes of uranium sink into the liquid outer molten core? An attentive reader will also be surprised how a 100-kilometer asteroid was able to successfully penetrate through the upper and lower mantle, the total thickness of which is ~2800 km.

Later, in 2016, the author suggested in [14] that the Moon separated from the Earth when it collided with a small comet. By analogy with previous hypotheses, this hypothesis has been called the Comet Impact Hypothesis (CIH). In [14] it was also shown that the comet only initialized nuclear processes, bringing the terrestrial multi-layers reactor out of thermodynamic equilibrium. Hence, in fact, the CIH hypothesis is a hybrid impact-fission hypothesis. Note that developed within the CIH hypothesis's framework the Elemental Buoyancy Theory (EBT) has allowed solving a number of problems and answered a number of geophysical questions.

Despite the obvious crisis associated with the absence of any chemical markers for the presence of the hypothetical planet Thea, some researchers after 2016 are

trying to save the giant impact theory by modernizing it [51]-[56]. Details and discussions about the several up-grade impact hypotheses such as a canonical single-impact, hit-and-run impact, fast-spinning Earth impact, general high-angular momentum and high-energy impact, and multiple impacts hypotheses could be found in reviews Rufu *et al.* [57] and Canup *et al.* [58], and works cited in them.

2.3. The Internal Structure of the Earth

In [14] [15] and [16] the Elemental Buoyancy Theory (EBT) was developed and it allow to explain the internal structure of the Earth. The structure of K-[Sr]-Cs-[Pb]-Th-U is determined by the buoyancy of the fuel isotopes and their main decay products. The levels that can degenerate due to the peculiarities of convective processes at different stages of the Earth's evolution are marked in parentheses. In its current state, the planet Earth is characterized by a three-level system of K-Cs-Th-U distribution of magmatic mass (more precisely, high-temperature plasma), which corresponds to the modern division into upper and lower mantle, outer and inner core. In [14] [15], it was predicted that the dominance of shallow or deep convection depends on the vertical stratification of igneous masses.

It was also shown that the nuclear ^{40}K fuel layer, located at a depth of 660 km, is the basis of a new volcanological and seismological theory, revision of the theory of subduction and continental drift, the origin of water, oils, and diamonds, the Moon-Earth viscous stream-droplet separation, a new elemental buoyant theory of inner structure of planets and stars, and finally, this ^{40}K fuel layer is an important milestone in the basic principles of creating habitable planets around stars nearby the Sun. Previously, the abstract concepts of inner structure of the Earth, and the theory of volcanic eruptions, earthquakes, and subduction received a clear and simple physical explanation.

In this work, it is shown that the multilayer nuclear internal structure, determined by the buoyancy law, significantly affects the process of ore formation on Earth and on the Moon.

2.4. Nucleogenesis and Ores

It is necessary to separate the theory of ore formation and the theory of the origin of chemical elements. The theory of the origin of elements is the theory of the synthesis of these elements in the bowels of natural stellar reactors or in the scientific reactors. The theory of ore formation is a theory describing the spatial and temporal placement of ore deposits on the surface of a planet or its satellite.

In nature, the dying low-mass stars, exploding massive stars and white dwarfs, as well as merging neutron stars are sources of chemical elements [59] [60]. These theories could also be called as B^2FH and K^2L models. In astrophysics, it is commonly believed that our star, the Sun, is a weak reactor that can create only light elements, mainly hydrogen and helium. Therefore, the above-mentioned

classes of star systems provide us with a variety of chemical elements found on Earth.

According to the B^2FH and K^2L models, the metallization of stars, including our Sun, occurs due to the transfer of heavy elements synthesized by powerful reactors located on neutron stars. So, first of all, we are interested in checking the transfer for presence of uranium and decay products, such as iodine and cesium. However, the author is surprised to find that the transfer equation is missing in the galaxy chemical models (GCE). Note that for 80 years of the existence of GCE models, none of the astrophysicists have asked a question about the transfer equation. The error is visible even in the name of the Galactic Chemical Evolution (GCE) models, so these models are not models of Galactic Chemical Transport (GCT). Thus, "*cunning exoplanet aliens*" somehow mysteriously brought chemical elements from different stars to the Earth and hid them in the form of concentrated ore deposits in the oldest terrestrial geological faults.

In Section 2, we briefly reviewed already known hypotheses; we stopped at the consideration of already known hypotheses; in the following Sections 3 and 4 we begin to develop the theory of ore formation.

3. Theory of the Origin of Earth ores

3.1. The Origin of the Earth Ores

As it was emphasized above, by about 2010 it was realized that the absence of any geochemical markers of the existence of the mythical planet Thea led to the rejection of the giant impact hypothesis (GIH). In the work [14] it was shown that our protoplanet collided not with the massive planet Thea (TIH, Thea Impact Hypothesis), but with a small comet (CIH, Comet Impact Hypothesis). In this study, we will present in more detail the process of formation of massive ancient terrestrial and lunar supercontinents, as well as the process of ore formation.

A comet impacted into the protoplanet at a grazing angle; this process is schematically shown in **Figure 2(a)**. It is assumed that by the time of impact, the process of vertical stratification of chemical elements inside our protoplanet was completed, so light elements rose to the surface, and heavy elements sank into the deep layers of the protoplanet. At the same time, the surface of the protoplanet cooled to such an extent that a protoplanetary crust formed on it.

Note that the process of formation of the protoplanet crust could have ended not earlier than 1 - 2 billion years ago. The ^{40}K nuclear layer forms a reverse thermocline, which prevents convection from the lower mantle layers and, accordingly, prevents the enrichment of the upper layers with heavy elements, see EBT model [14]. Therefore, the crust of the protoplanet was formed as a result of cooling of mainly light elements, that is, elements with atomic numbers $z < 19$ (K, $z = 19$). Accordingly, there were no heavy metal ores on the surface of the protoplanet. Due to the principle of minimizing potential energy, the shape of the protoplanet was spherical, or rather, due to rotation, most likely ellipsoid. That is, the topography of the Proto-Earth had unimodal behavior, the same as

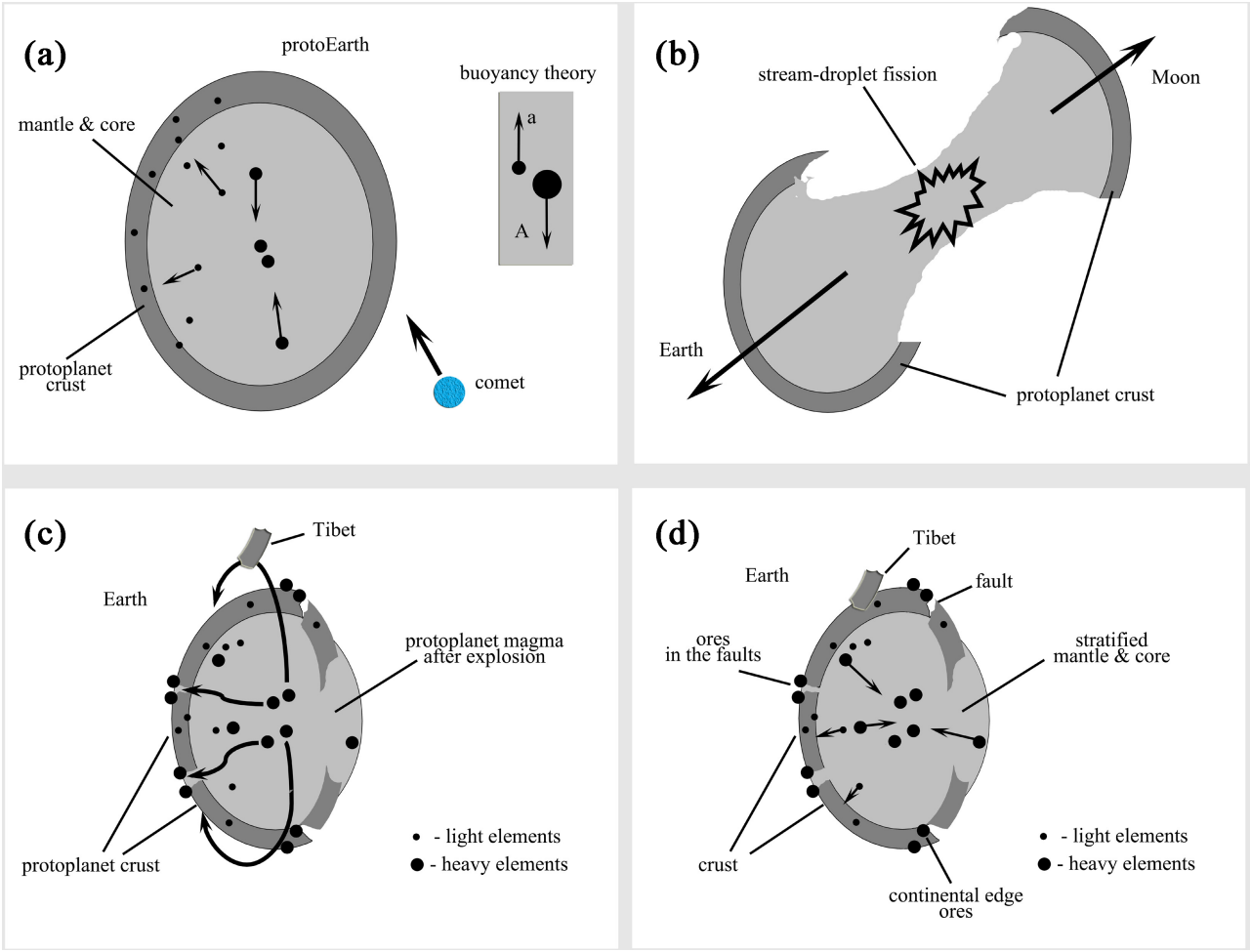

Figure 2. The scheme of ore formation on the Earth's surface after a collision with a comet is presented as a four-stage process. (a) A comet hits a protoplanet at a sliding angle to its surface; (b) thermal nuclear explosion after a collision with a comet. The formations of the Earth and the Moon are the result of the viscous stream-droplet separation process; (c) the process of flow up of heavy elements from the deep layers of the planet; (d) the origin of ores is the result of solidification of heavy elements in the old geological faults, as well as near the edges of the ancient monoblock continent. In all Figures (a)-(d), the pieces of protoplanetary crust are filled by dark gray, light gray color corresponds to the magmatic mass of the mantle-core. Additionally, the plate of Figure (a) illustrates the elemental buoyancy theory (EBT) in the form of a simple separation scheme.

the topography of Venus at the moment.

A small comet, consisting mainly of carbon dioxide ice, got into a hot ^{40}K nuclear layer that led to a thermal nuclear explosion. A viscous stream-droplet separation of the protoplanet into two parts occurred with the formation of a constriction ("*navel-string*"); this process is illustrated in **Figure 2(b)**. This type of division was predicted in 1879 by the grandson of the famous evolutionist G.H. Darwin [27]. However, due to the lack of information at that time about the nature of nuclear interactions, G.H. Darwin could not correctly indicate the cause of such a separation

Note that as a result of the stream-droplet separation, the chemical composition of the Earth and the Moon must be identical, since the planet and satellite were formed from the material of the same protoplanet. However, note that the

Moon is formed mainly from material located in the upper layers of the protoplanet, so the density of the Moon is much less than the density of the Earth.

In addition, the Moon, like the Earth, received a large supercontinent from the protoplanet; please see the dark gray areas in **Figure 2(b)**. The lunar continent did not split and did not undergo changes in the future, so the lunar supercontinent remained on the far side of the Moon, invisible from the Earth. The near and far sides of the Moon are very different from each other, which is in good agreement with the concept of stream-droplet fusion. In particular, the near side of the Moon is once completely melted surface. The topography of the Moon and Earth has become bimodal, which is typical for planets and satellites that have suffered serious damage during the collision and after it at the cooling stage.

Immediately after the separation of the Moon, due to the increase in pressure during the explosion of the thermal nuclear layer ^{40}K, but with a slight delay, the lower Th-U layer, lying deepest near the center of the protoplanet, detonated (**Figure 2(c)**). The supercontinent of the Earth, formed from the crust of the protoplanet, lifted and cracked. Hot magmatic flows from the deep layers of the planet poured into the cracks, as well as through over the edges of the continent. These streams were enriched with heavy elements (see the location of large spots in **Figure 2(c)**).

Therefore, the first group of ores was formed by igneous rocks that got stuck during cooling in the geological faults of a single but cracked supercontinent. Another group of ores are formed as a result of the overflow of magma enriched with heavy elements over the edge of the supercontinent. Later, the heavy elements remaining in the molten liquid magma, under the influence of the law of buoyancy, began to sink into the deep layers, while the light elements that appeared as a result of the explosion on the bottom layers, gradually began to float up. This process of ore formation is schematically presented in **Figure 2(d)**.

During the explosion, the vertical stratification was destroyed, which leads to the dispersion of thermal nuclear layers. The scattering of nuclear layers leads to a decrease in their heat release, which, in turn, leads to a sharp cooling on the Earth. Thus, we get the opportunity to clarify the dating of the collision with the comet, given earlier, basined on the time factors of the formation of the protoplanet crust. To do this, we will use the standard International Chronostratigraphic Table, v2020/03 [61] [62].

As shown in the ICC Table, a sharp cooling of the Earth occurred at the beginning of the Cryogenian, at 0.72 Ga. On the other hand, the single Rodinia terrestrial super continent disintegrated ~0.75 Ga. Therefore, taking into account the accuracy of the ICC 2020 itself, the formation of the Moon-Earth system occurred in the interval of 0.72 - 0.75 Ga. It should also be noted that the formation of water occurred quickly, as a result of a nuclear reaction, under the crust of the planet, almost simultaneously with the formation of ores [14]. Thus, the Tonian duration, 0.72 - 1.0 Ga, is greatly overestimated.

3.2. Enrichment of the Earth's Surface with Ores during the Galactic Storms

To the process of ore formation described in Section 3.1, we should add the process of enrichment with intermediate elements (approximately $30 < z < 80$) during the evolution of our planet. In 1912, Alfred Wegener, a German climatologist, geologist, geophysicist and meteorologist, proposed the theory of continental drift. Thus, A. Wegener was the first to suggest that the Earth is undergoing significant structural changes in the process of evolution. An overview of the works devoted to the relationship of galactic processes with structural changes, which are often accompanied by mass extinctions and continental drift, can be found in [15].

According to [14], within the framework of the theory of buoyancy (EBT), thermal gradients corresponding to the boundaries of the K-[Sr]-Cs-[Pb]-Th-U mantle-core structure, in a calm, undisturbed state of the Earth, prevent the occurrence of deep convection and enrichment of the overlying layers with heavy chemical elements lying below, in the depth of our planet. In particular, the presence of a thermocline formed by a ^{40}K hot nuclear layer at the boundary of the upper and lower mantles determines the fact that during this period of the Earth's evolution, volcanic lavas, as well as volcanic gas and ash contain only light chemical elements with atomic numbers below this potassium ($z < 19$). However, under the influence of gravitational compression of the galaxy, activation of nuclear layers formed thermoclines, and disturbance of vertical stratification can occur [15].

The scheme of enrichment of the earth's lithosphere with intermediate chemical elements during the change of the magmatic convection regime from shallow to deep is shown in **Figure 3**. The state of the planet before the galactic storm is schematically shown in **Figure 3(a)**, during the galactic storm—in **Figure 3(b)**, and immediately after the galactic storm—in **Figure 3(c)**.

Unlike the comet impact that led to the destruction of the protoplanet (**Figure 2**), the galactic impact observed in the past did not lead to the destruction of the planet, but was accompanied by a sharp and sudden warming at the boundary of geological epochs, followed by a deep cooling. Under this influence, the viscosity of magma decreases, and continents can move under the action of jet magmatic currents (**Figure 3(b)**). As a result of one of these galactic impacts, the Middle Ocean Ridge Basalts (MORBs) and Large Igneous Provinces (LIPs) were formed. In the same way, during a galactic storm, vertical stratification is disrupted, and intermediate elements can rise up and reach the areas of the MORBs and LIPs.

The process of formations of MORBs and LIPs should have a pronounced character, accompanied by rapid heating of the nuclear layers under loading, followed by slow deep cooling during the dissipation of thermal nuclear layers. The dissipation of thermal nuclear layers will lead to cooling, later under the influence of the law of gravity, heavy elements will again start sink down and light elements will begin to rise up. Thus, during the entire galactic storm there will

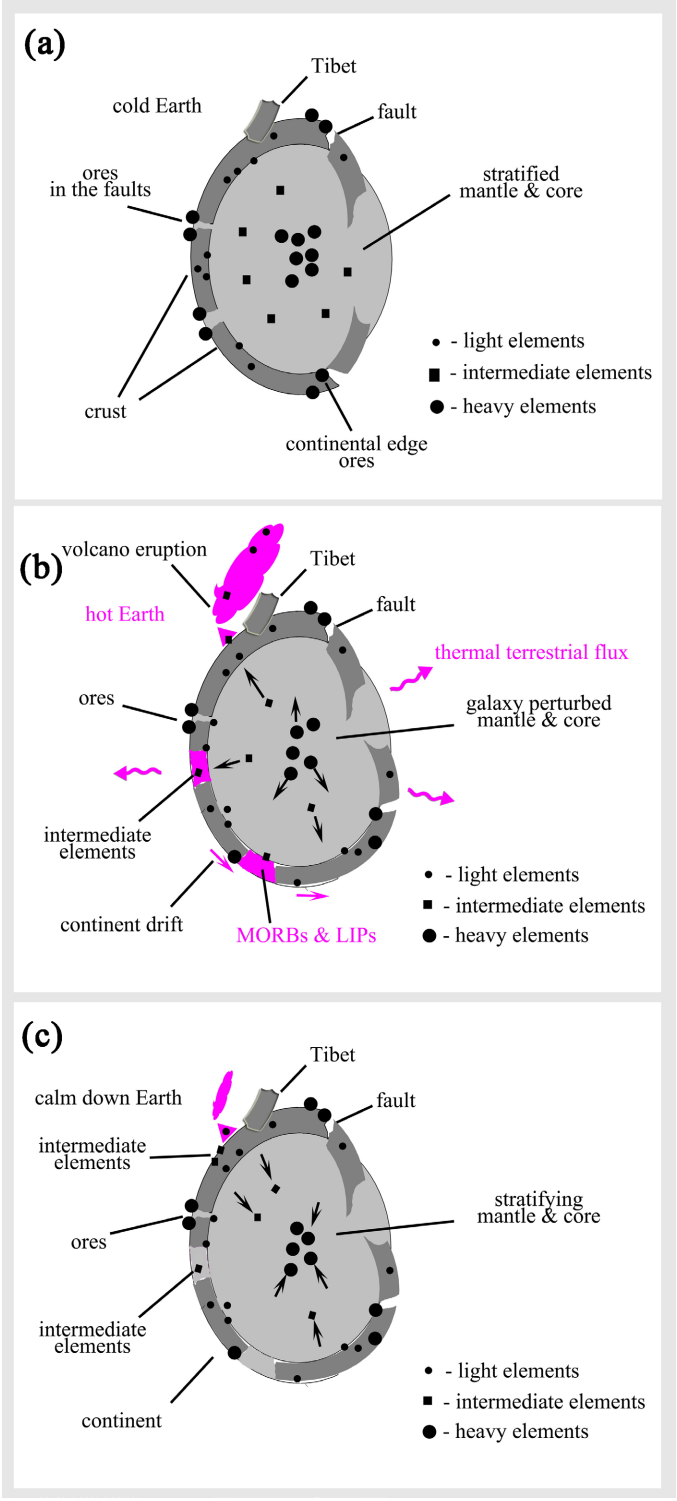

Figure 3. The process of enriching the Earth's lithosphere with chemical elements is presented. (a) The stage of galaxy calm. The inner mantle-core terrestrial structure is stratified; (b) the stage of galaxy storm. The internal structure of the Earth's mantle-core is perturbed, the Earth is hot, and the continents are drifting. Intermediate elements can be found in the sediments of the seabed and present in the MORBs and LIPs; (c) the end of the galaxy storm. The internal structure of the Earth's mantle-core begins to stratify. The intermediate and heavy elements are lowered down.

be a process of heating and cooling of the planet, as well as an increase and decrease in the ocean level, while these processes will have a pronounced sawtooth character.

At the end of the galactic storm, intermediate elements that are not get stuck in MORBs, LIPs, or are not deposited in volcanic ashes and lavas will slowly sink down to their original state, and the initial vertical stratification will be established (**Figure 3(c)**). The galactic process of ore formation by enrichment with intermediate elements described in this section is of a smaller scale and is secondary in comparison with the process of ore formation in a collision with a comet.

4. Theory of the Origin of Lunar Ores

As well known, the topography of the Moon has a bimodal distribution, while the far side of the Moon is elevated above the zero (ground) level of the surface. This distribution is typical for planets and satellites that are strongly affected by cosmic bodies at late stage of their cooling [14]. Moreover, there is a giant crater on the far side, the size of which is incompatible with the existence of the Moon itself, so this crater only can occur during the formation of the Moon. Earlier in [14], it was suggested that this crater is a crater from a comet that hit the original protoplanet, and, accordingly, the lunar continent on the far side of the Moon is part of the protoplanet's crust.

Based on the concept of a thermal nuclear explosion and viscous liquid stream-droplet separation, one of the well-known paradoxes of the Moon is immediately solved, which is that the near side and far side of the Moon are very different from each other. The process of formation of the Earth and the Moon as a result of the liquid stream-droplet separation is clearly shown in **Figure 4(a)**.

The lunar surface on the nearside is an ocean of molten magma. Due to the presence of an ocean of molten magma, the number of meteorite craters on the near side is significantly less than on the far side. Despite the huge areas covered with magmatic lavas, there are no classical cones of volcanoes typical of terrestrial geology in the near side. Thus, the lava formations on the nearside are formed not by volcanic activity, but by other processes.

According to the author's hypothesis [14], pieces of protoplanet crust and other cosmic bodies, such as meteorites, if they fall into the molten ocean of lunar magma on the near side of the Moon, then sink into the depths. Thus, the hypothesis proposed by the author solves the paradox of the discrepancy between the molten mass and the absence of significant meteoritic and volcanic lunar activity on the visible part of our satellite.

Next, let's look at the far side of the Moon. The greater number of meteorite craters on the far side of the Moon is explained by the fact that due to the lunar crust on the farside (the lunar continent) formed from a single piece of protoplanetary crust, traces of bombardment will always remain, regardless of whether

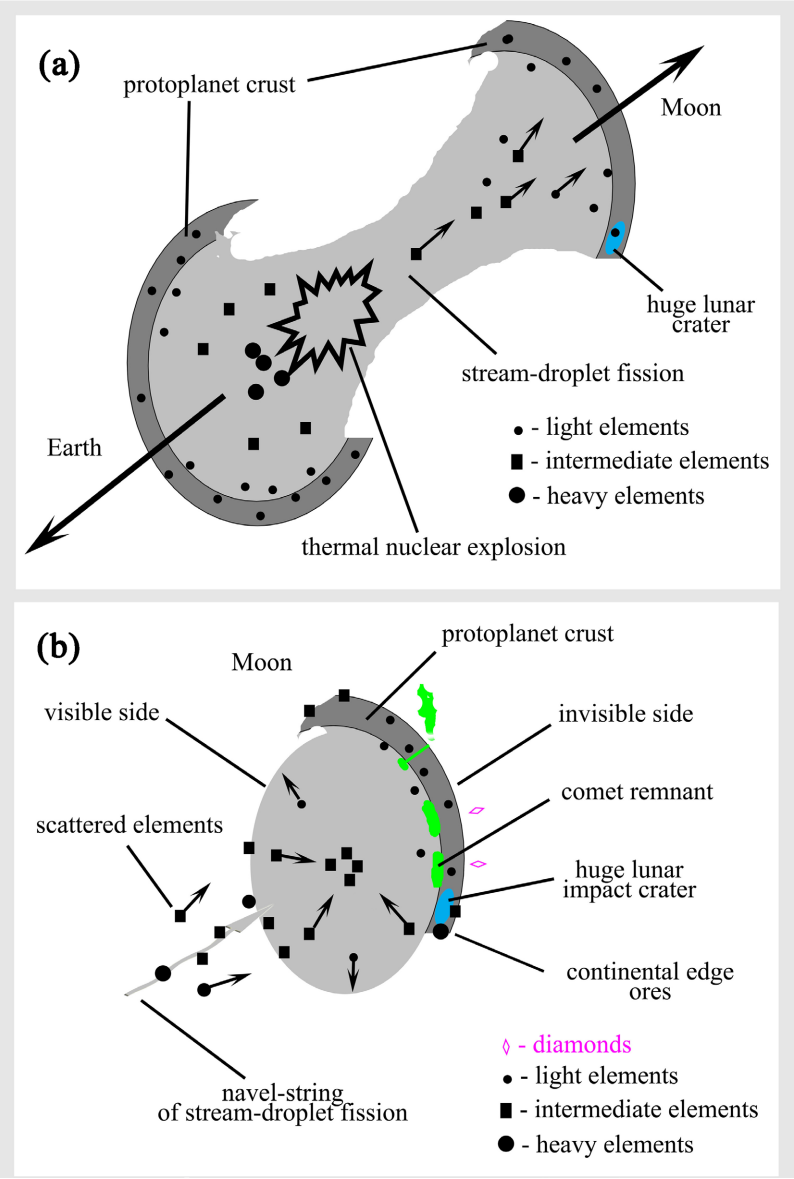

Figure 4. The scheme illustrates the process of formation of lunar ores. (a) Thermal nuclear explosion of a protoplanet after a collision with a comet. The Moon was created as a result of the viscous liquid-droplet separation from a piece of crust and the magmatic mass of a protoplanet; (b) the stage of cooling of the Moon and the formation of lunar ores. The huge lunar comet impact crater is filled by blue sport; the gaseous comet remnants under the crust are green; diamond deposits are shown by violet rhombuses, and the lunar volcano spews a gas plume which is also drawn in green as some comet remnants.

this lunar continent was covered with a thin layer of molten magma that overflowed over the edge of this continent, or no.

Further, we will focus on the process of formation of lunar ores, that is, we will try to find an answer to the question of what ore formations can be found on our satellite and whether it is advisable to develop them.

The process of formation of the lunar ores is schematically shown in **Figure 4(b)**.

Due to the sliding impact of the comet into the ^{40}K nuclear layer, the explosion of the uranium layers occurred sluggishly after the separation of the Moon. The Moon was formed mainly from light and intermediate elements, which explains why the density of the Moon is much less than the density of the Earth. Due to the nature of the explosion, chemical elements heavier than potassium will be present on the Moon in limited quantities, see **Figure 4(a)** and **Figure 4(b)**. Secondly, due to the absence of faults on the far side of the lunar continent, ores can only be represented on the Moon by ores of the overflow nature of the formation. All intermediate and heavy elements that have landed on the near side of the Moon are not stuck on its molten surface and will rather quickly sink into the depths of the satellite under the influence of gravity (**Figure 4(b)**).

And the last thing I would like to pay attention to is the formation of some geological feature in the middle of the near side of the Moon. With liquid-droplet separation, this usually leads to the formation of a constriction between the two parts. This constriction will lead to the formation of a geological feature (navel-string) in the center of the visible part of the Moon, please see **Figure 4(a)** and **Figure 4(b)**. Note that this region may be enriched with heavy elements due to the central part of stream-droplet flow (navel-string), which managed to cool down in flight and landed to the surface of the Moon with a significant delay.

5. Spatial Distribution of Chemical Lunar Elements

5.1. The Lunar Spatial Distribution of Nuclear Abundances

This section examines the content of some elements on the Moon, which were obtained using the Lunar Prospector Gamma Ray Spectrometer [21]. The abundances of potassium (K) and thorium (Th) in ppm are shown on the near side (**Figure 5(a)**) and the far side (**Figure 5(b)**) of the Moon. In this study, the data of the Prospector were presented in an orthographic projection of the Moon. Recall that the different Prospector abundances have different spatial resolutions. In particular, the spatial resolution of potassium was equal to 2˚, and thorium—0.5˚ per pixel.

The study of the spatial distribution of chemical elements on the Moon showed the following. Firstly, on the near side of the Moon the concentrations of these elements are much greater than on the far side of the Moon. On the far side, a slight increase in concentrations is observed only near the giant impact crater. On the visible side of the Moon, the spatial distribution of potassium is wider than for thorium, but the general shape of these distributions is the same. Secondly, the distribution of thorium, as we expected, is presented in the form of a whip. Recall that such a distribution was formed as a result of the stream-droplet Earth-Moon separation, please see **Figure 4** band **Figure 5(c)**. Previously, this distribution was called the navel-string.

Further in this work we investigated the cross-section distributions of abundances along the lunar near-side equator. For ease of presentation, smoothing

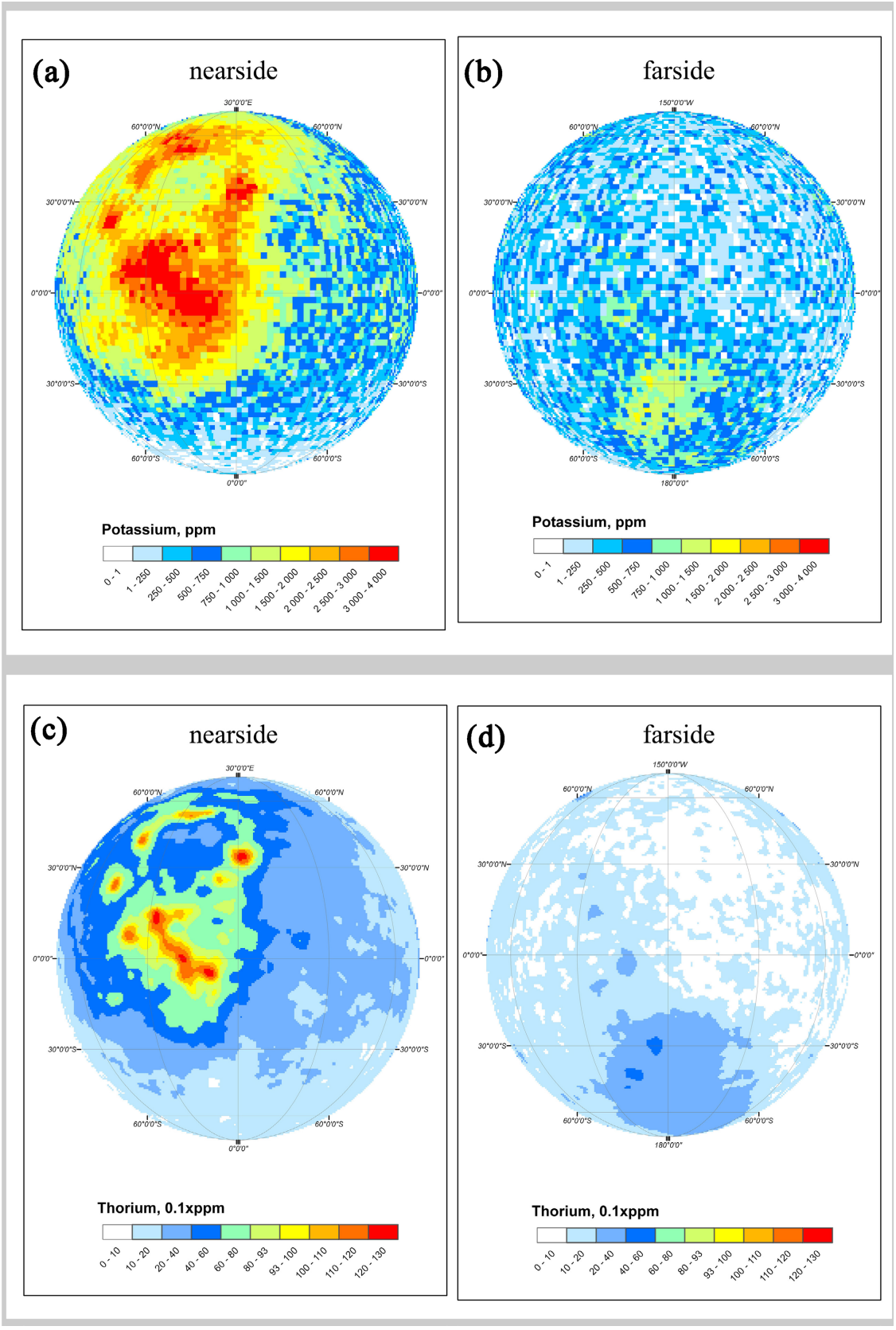

Figure 5. The spatial distributions of potassium (2˚ per pixel) and thorium (0.5˚ per pixel) abundances are shown on the nearside (a) and the farside (b) of the Moon.

was additionally applied; the data with a resolution of 2˚ in pixel was smoothed by 10 points and with a resolution of 5˚ smoothing by 20 points. The equator cross-section distributions of potassium, thorium and silicium abundances are shown in Figure 5. The cross-section distribution of thorium and potassium shows a good agreement; see Figure 5(b). According to the author, a high degree of agreement between these distributions is associated with the process of activation of a thermal nuclear explosion, when the upper layer of ^{40}K detonated first, and then the lower Th–U nuclear layers were detonated.

In this situation, it is of interest to compare the distribution of thorium with the distribution of silicium (Si, z = 14), which is a light element and is part of the rocks that define the presence of the protoplanet crust. A comparison between the near-side equatorial cross-sections of silicium and thorium is shown in Figure 6(a). The silicium cross-section distribution is in antiphase to thorium. Since such a spatial distribution of thorium, potassium and silicium, it can be concluded that the process of destruction of the silicium layer, from which mainly consists the lunar crust, occurred during the explosion, this confirms the nature of the process of the Earth-Moon separation, shown above in Figure 4(a).

5.2. Lunar Spatial Distribution of Lightweight Elements

In this section, we will conduct studies similar to those described in the previous section, only for titanium (Ti, z = 22) and iron (Fe, z = 26). Both of these elements are relatively light, but due to the fact that these elements are heavier than potassium, which forms a thermocline layer during the stratification of magmatic masses, these elements are significantly less represented in the protoplanetary crust.

The spatial distributions of TiO_2 (2˚ per pixel) and FeO (0.5˚ per pixel) abundances obtained by the Lunar Prospector Gamma Ray Spectrometer are shown on the lunar near side (Figure 7(a)) and the far side (Figure 7(b)). In general, the spatial distributions of these elements are similar to the distributions presented earlier, that is, a lot of matter was sprayed over the visible part of the Moon and much less over the back side of the satellite, mainly in the area of the giant impact. The latter is a consequence of the ejection of a certain amount of matter from the hole formed when the comet entered the protoplanet. The ejection is directly opposite to the trajectory of the comet's fall.

The near-side equator cross-sections of the distribution TiO_2 and FeO abundances are shown in Figure 8. Next, it is of interest to compare the distribution of iron and calcium (Ca, z = 20); these spatial distributions are shown in Figure 8(a). A comparison of the equatorial cross-section of calcium and iron shows an antiphase behavior. Note that the similar antiphase behavior with Ca vs Fe (Figure 8(a)) or Si vs Th (Figure 6(a)) is not observed for magnesium (Mg, z = 12) and aluminum (Al, z = 13), which are lighter than potassium (K, z = 19) and, accordingly, according to the theory of standard stratification, are located above

the ^{40}K thermocline, forming the boundary between the upper and lower mantle. As shown in Figure 8(b), the cross-section spatial distributions of titanium and iron are in good agreement.

5.3. Lunar Spatial Distribution of Heavyweight Elements

In the dataset obtained by the Lunar Prospector Gamma Ray Spectrometer, heavy elements are represented only by abundances of samarium (Sm, z = 62)

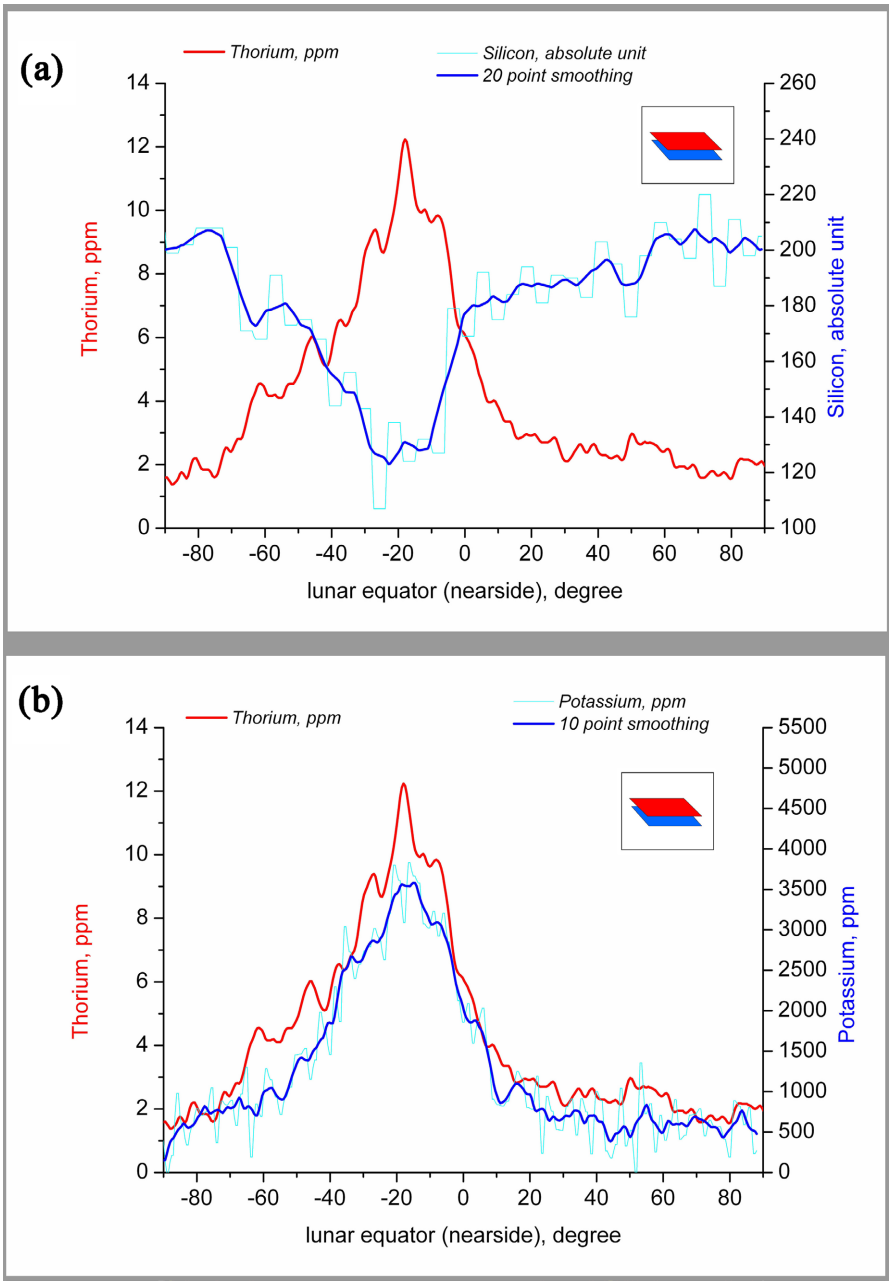

Figure 6. The cross distributions of silicon (2˚ per pixel), potassium (2˚ per pixel) and thorium (0.5˚ per pixel) abundances are shown along the equator of the near side of the Moon. The spatial distributions of thorium-silicon in (a) are in the opposite phase, while the spatial distributions of titanium-potassium show a good agreement, see (b).

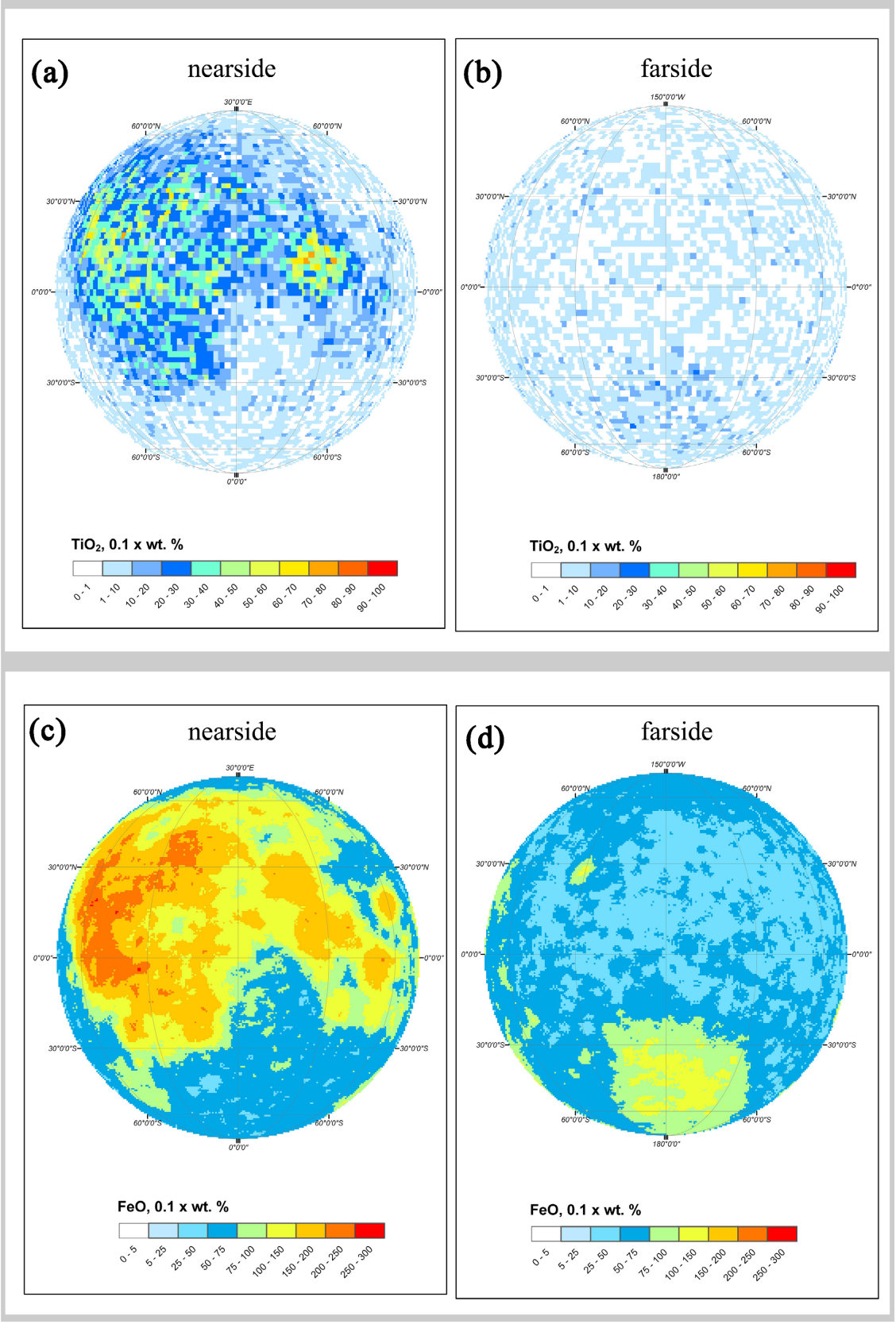

Figure 7. The spatial distributions of TiO_2 (2˚ per pixel) and FeO (0.5˚ per pixel) abundances are presented on the lunar nearside (a) and farside (b).

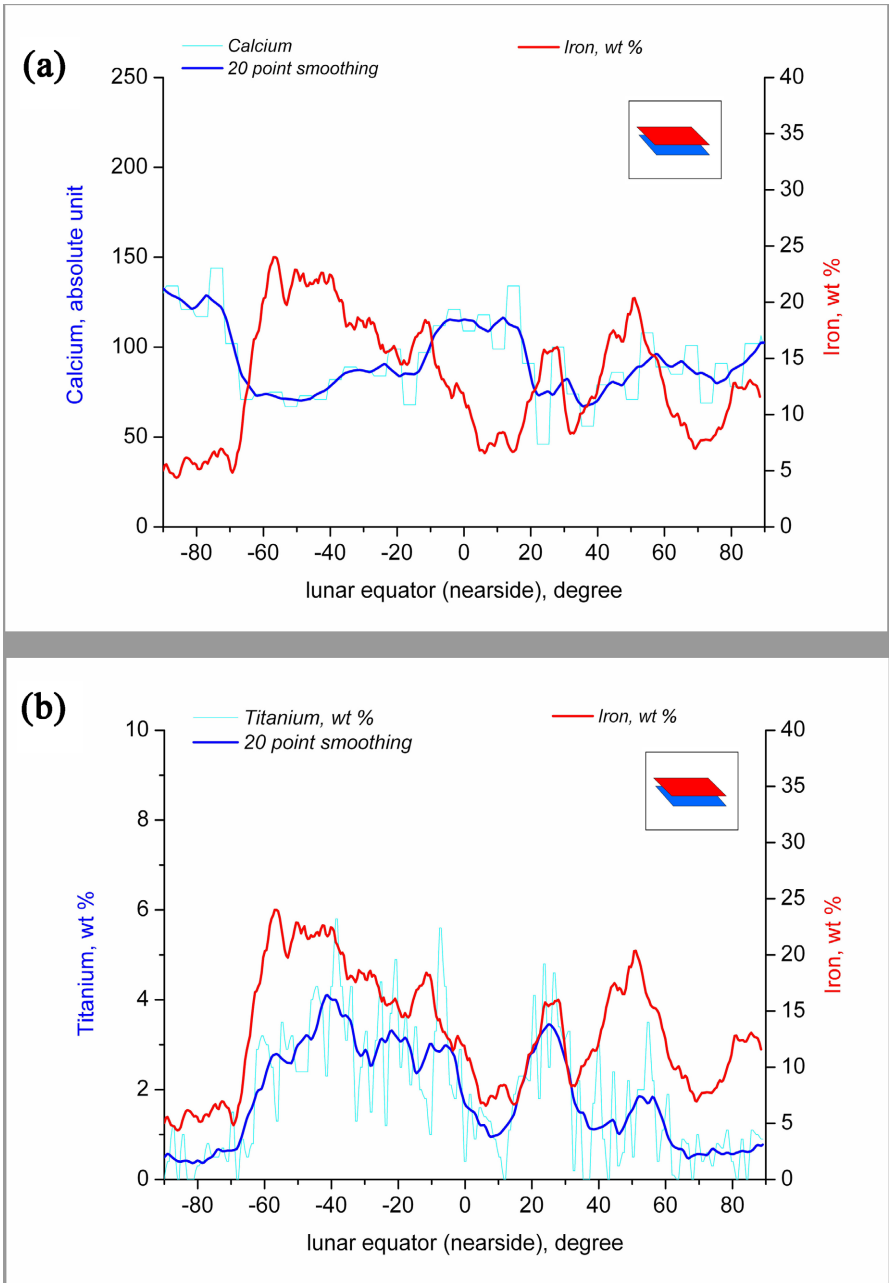

Figure 8. The near side equator cross-sections of distribution of calcium (5˚ per pixel), TiO_2 (2˚ per pixel) and FeO (0.5˚ per pixel) abundances are shown in (a) and (b). The calcium-iron spatial distributions in (a) are in the opposite phase, while the titanium-iron distributions show good agreement, see (b).

with a resolution of 2˚ per pixel and thorium (Th, z = 90) with a higher resolution of 0.5˚ per pixel.

In this study, the distributions of these elements were compared with the spatial distribution of iron. A comparison of the spatial distribution of Sm and FeO abundances on the near and far sides of the Moon is presented in **Figure 9(a)** and **Figure 9(b)**. As shown in this figure, the spatial distributions of samarium and iron are in the opposite phase, *i.e.* where there is a lot of iron, there is little

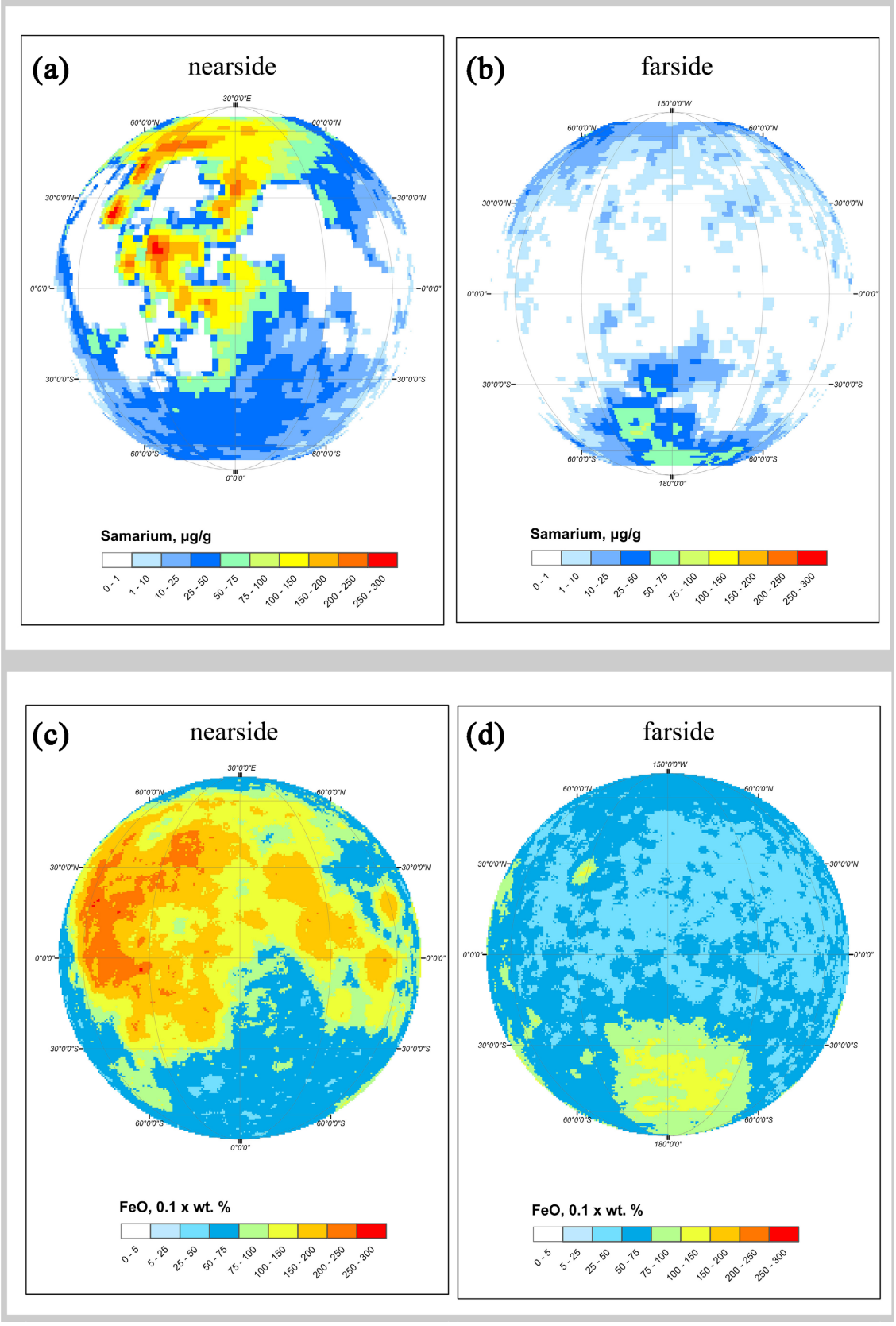

Figure 9. The comparison between the spatial distributions of Samarium (2˚ per pixel) and FeO (0.5˚ per pixel) abundances are presented on lunar near side (a) and far side (b).

samarium.

In Figure 10(a) in the orthogonal projection of the Moon shows the nearside equatorial cross-section distributions of samarium and iron abundances, obtained, as indicated above, using the data set of Lunar Prospector Gamma Ray Spectrometer and ArcInfo GIS method. The spatial distributions of samarium and iron have the opposite behavior, Figure 10(a). The opposition of the two distributions is not only general, but also coincides up to individual extremes, marked on Figure 10(a) in the form of vertical dotted lines. However, the spatial distributions of samarium and thorium depicted in Figure 10(b) show synchronization of

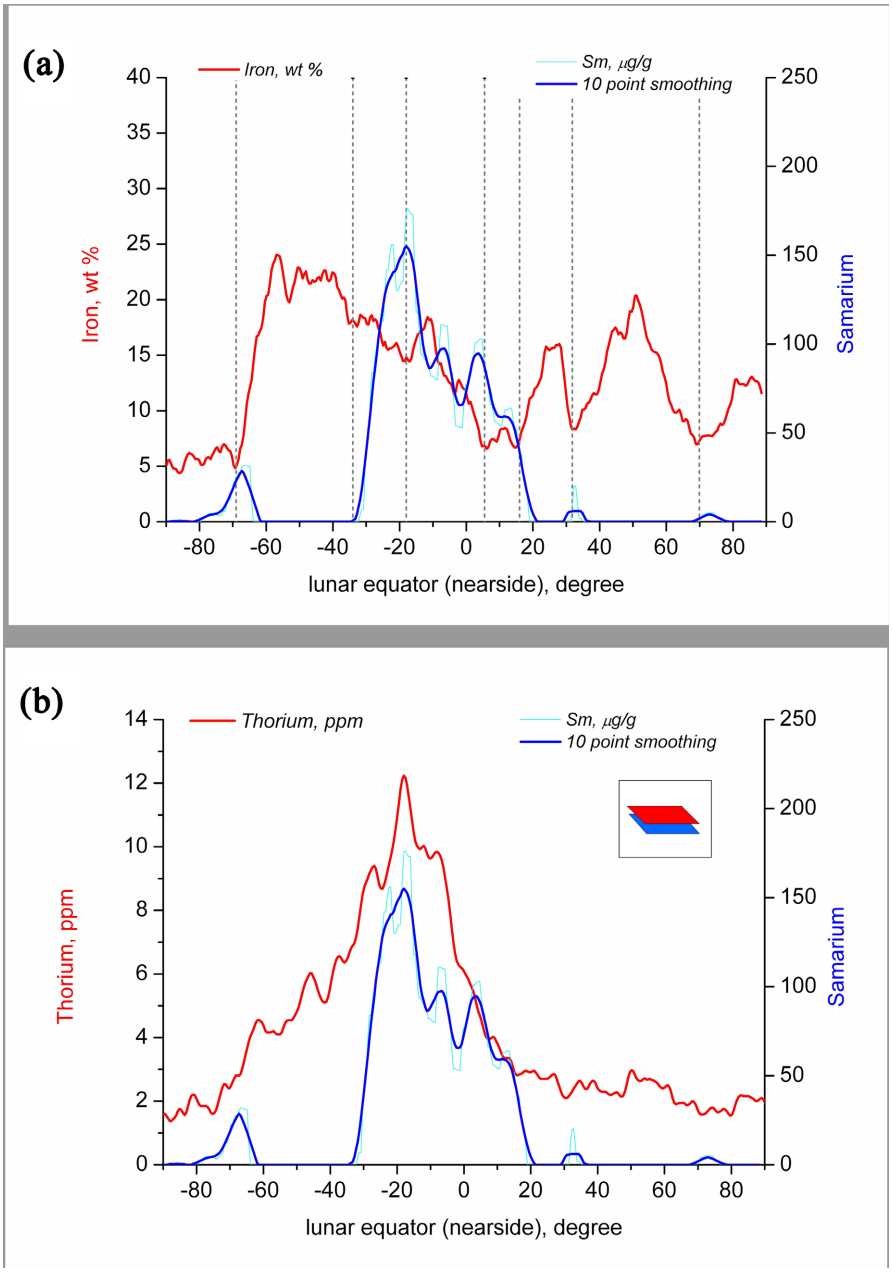

Figure 10. The cross distributions of Thorium (0.5˚ per pixel), Samarium (2˚ per pixel) and FeO (0.5˚ per pixel) abundances are shown along near side equator of the Moon.

maxima in the lunar longitude range from −30˚ to 20˚.

Let's summarize the above. Thus, closer to the navel-string (**Figure 4(a)**), as expected, heavy elements predominate, which settle in an inverse order, first lighter, then heavier, that is, in the sequence in which they burst out of the central region of the protoplanet. At the periphery of the constriction, moderate and light chemical elements predominate, located near the border of the upper and lower mantle of the protoplanet. Due to their spatial location in the protoplanet crust, these moderate and light elements are more widely scattered over the surface on the near side of the Moon and, as we have shown above, can partially overlap the layers of heavy elements due to the fact that their ejection from the provincial regions of the protoplanet occurs with a slight delay. A separate class is the distribution of elements on the far side of the Moon, in the area where the comet broke through the crust of the protoplanet.

6. The Terrestrial and Lunar Volcanic Eruptions

6.1. Theory of Terrestrial Volcanic Eruptions

The paper [16] presented a new theory of volcanic eruptions on Earth. Since the earth and lunar surfaces could be enriching by volcanic eruptions, in this section, we investigate and compare volcanic processes occurring on the Earth and on the Moon. The new theory is based on the excitation of a ^{40}K nuclear thermal layer located at a depth of ~660 km, on the border of the upper and lower mantle [16]. A simple diagram of an intrusive volcanic eruption on Earth is shown in **Figure 11(a)**. In this type of eruption, the formation of a standard volcanic cone occurs due to the melting of the young crust in the subduction zone. According to the EBT theory, during the calm period of the galaxy, characterized by stable vertical stratification, the compounds containing chemical elements lighter than potassium should dominate in magmatic terrestrial lavas and plumes. The hot ^{40}K layer, in which the young crust of the planet melts, plays the role of a thermocline that prevents the rise of elements heavier than potassium, such as Ni and Fe, in the terrestrial volcanic ashes and magmatic lavas.

Thus it is naive to sit at the mouth of a volcano and wait for lava to flow out of it, enriched with gold, silver or platinum. With stable stratification, this will not happen. And the last note: the angle of inclination of the subduction plate determines the spatial location of the volcano ridge near the edges of the earth's continents, as shown in **Figure 11(a)**.

6.2. Theory of Lunar Volcanic Eruptions

Next, let's consider how things are with volcanic activity on the Moon. The absence or decrease in the amount of uranium, as well as the low density of magma, leads to the fact that the Moon has cooled down a lot and at the moment there is no volcanic activity on the Moon. The absence of subduction zones reduces the likelihood that volcanic activity similar to that observed on Earth has ever been observed on the Moon.

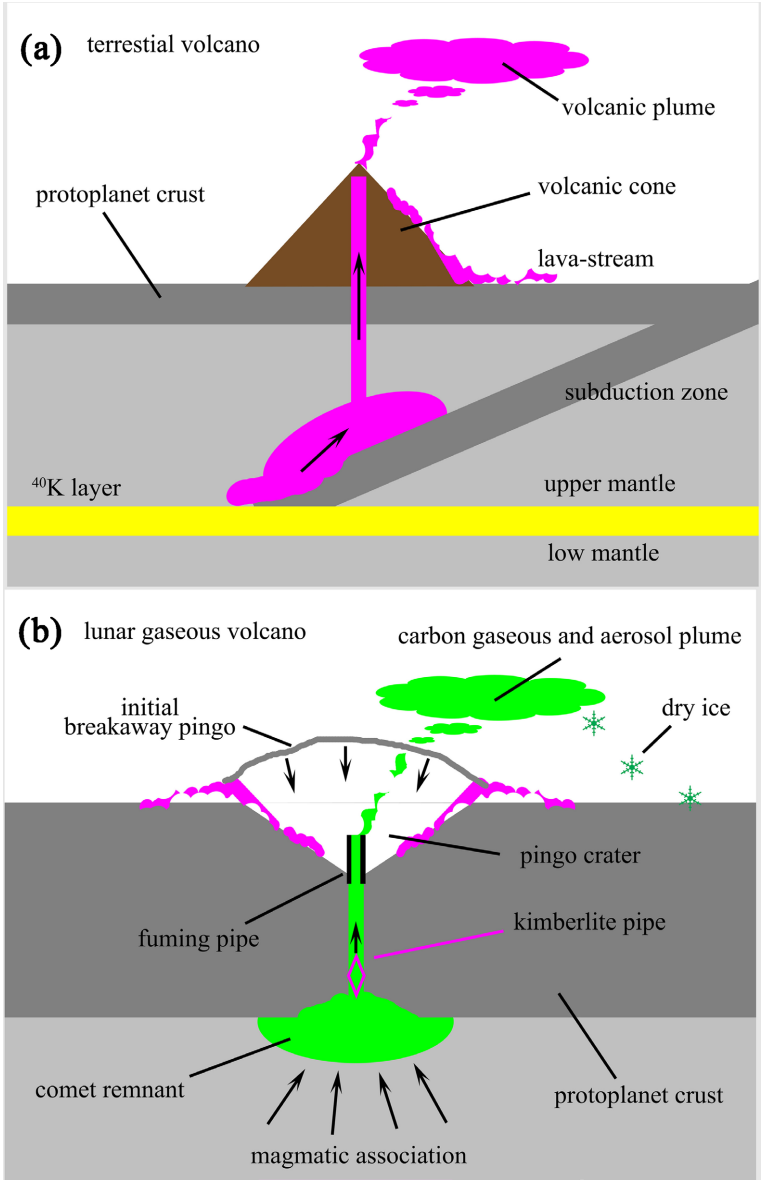

Figure 11. The comparison of volcanic processes occurring on the Earth and the Moon is highlighted. (a) The scheme illustrates the formation of a typical volcanic cone on Earth during the processes of crust melting in the subduction zone; (b) the formation of a reverse lunar volcanic cone on the far side of the Moon during the eruption of the remnants of a comet trapped under the crust of the lunar continent. A lunar volcanic crater might have an explosive feature with the synthesis of a kimberlite pipe and diamonds, or a smoking feature with the formation of a typical prominent fuming-pipe (usually a central peak) in the center of the lunar collapsed pingo crater.

On the other hand, powerful pseudo-volcanic activity was observed on the Moon, as well as on Earth at the time of their formation. By pseudo-volcanic activity, the author understands the geological processes associated with the entry of a comet consisting of carbonic gas under the lunar continent. The process of movement of the fragments of the comet under a lunar continent, which is a part of original protoplanet crust, is schematically shown in **Figure 4(b)** with

green dots.

Carbon dioxide trapped under the lunar crust as a result of the collision of a protoplanet and a comet tended to evaporate to form a convex basin, sometimes called a pingos. The processes of pingo collapse and the formation of an inverse lunar volcanic cone ("tall wine glass") are simplified in **Figure 11(b)**. Some information about the creation, evolution and collapse of terrestrial and Martian pingos can be found in [63] [64] [65] and references therein.

Depending on the pressure in the areas of accumulation of the comet remains, the process of gas outflow from the bowels of the Moon can be explosive or proceed in the form of a weak outflow of gas jets. Therefore, the lunar pseudo-volcanic process may have an explosive or effusive character. With the explosive behavior of a lunar pseudo-volcanic eruption, the formation of a "*kimberlite pipe*" and the synthesis of diamonds can occur. However, during an effusive lunar eruption, the volcanic flow of carbon monoxide and dioxide has a fuming behavior, and a steaming-pipe can be formed in the center of the lunar collapsed pingo crater. At lunar night, lunar carbonic gas freezes and precipitates as a dry ice. Also about carbon content and degassing history of the lunar volcanic glasses, please see [66] [67] [68], and references therein. In particular, Yokota *et al.* reported that observed emissions around lunar mares, such as Oceanus Procellarum, were substantially higher than emissions around highlands [69]. It was also reported that extraneous carbon supplies by solar wind and micrometeoroids are less than the ongoing outflow, and are not consistent with regional differences. This study emphasizes that the possible explanations for regional differences are internal factors, such as the distributions of C_2H_4 and CO_2 stored in the remnants of ancient lunar volcanism and the pathways of gas release from the internal reservoir.

We also remind that the probes obtained by Lunar CRater Observation and Sensing Satellite (LCROSS) impact, show that the CO_2 could be cold trapped and the impact plume from the lunar crater Cabeus also contained CO_2, please see [70] [71].

6.3. Lunar Pyroclastic Volcanic Deposits

Note that during the collapse of the pingos, magmatic lavas are released along the edges of the craters, which is an expected phenomenon. In [23] [24] the spatial distribution of lunar pyroclastic volcanic deposits and the locations of volcanic vents were investigated. This spatial distribution is represented in **Figure 12** in the form of colored triangles. The Kaguya topography of the two sides of the Moon [72] is additionally presented in **Figure 12**. As follows from this figure, volcanic vents (triangles) are located along the geological faults of the nearby mare-highland boundaries (grey dash lines), as well as at the bottom of some lunar craters.

In addition, as also follows from **Figure 12**, the topography of the near and far sides are very different. Thus, the lunar topography once again confirms the

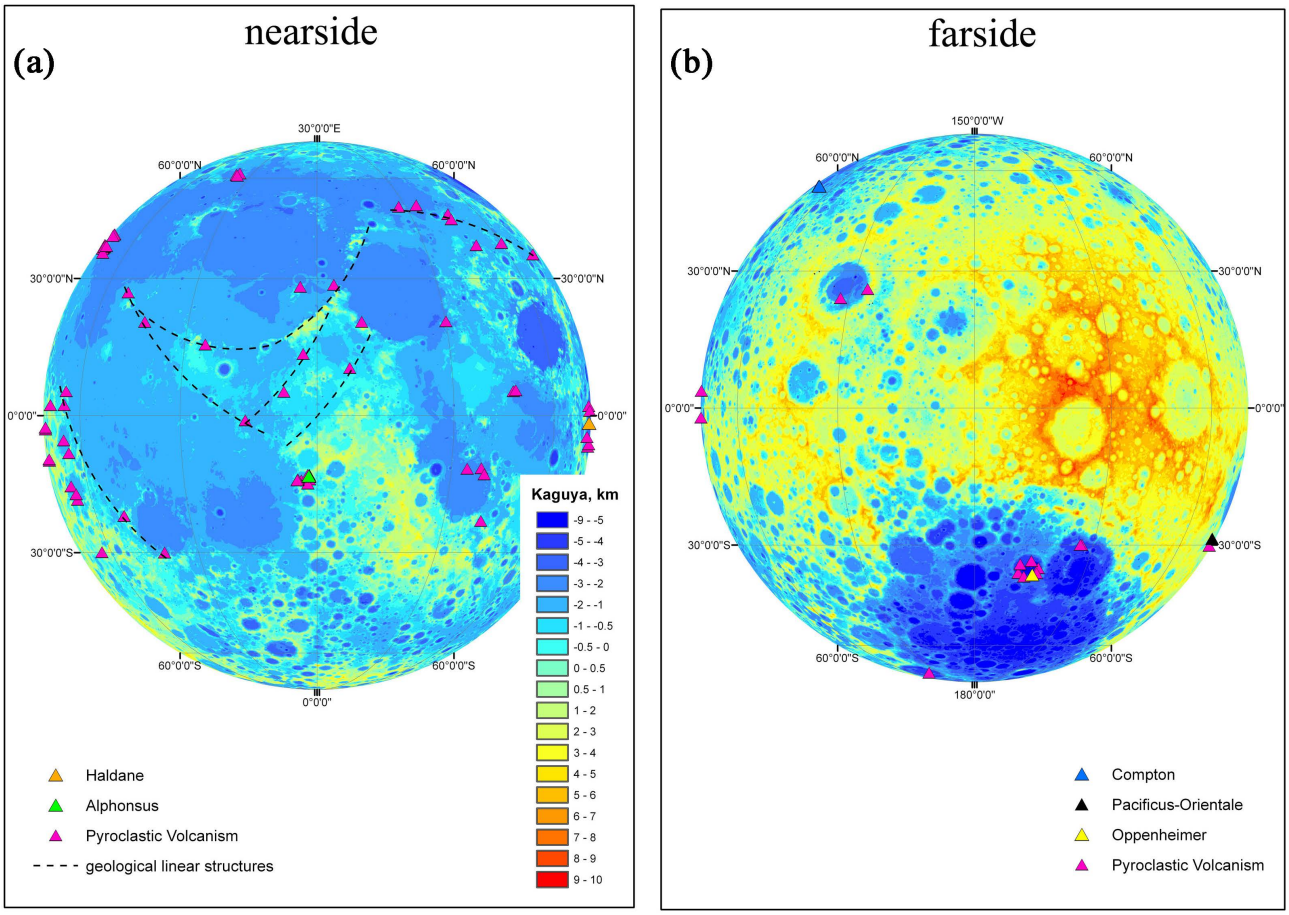

Figure 12. The topography of Kaguya on the near (a) and far (b) sides of the Moon is presented. Pyroclastic deposits are recorded along the geological linear structures (grey dash lines), as well as at the bottom of some crates (see margin triangles). Additionally, the craters Alphonsus, Haldane-Tasso S, Compton, and Oppenheimer, mentioned in the text of the manuscript, are marked with colored triangles.

hypothesis that a piece of protoplanet's crust falls within the back side of the Moon; please compare **Figure 12** with **Figure 2(a)** and **Figure 4(a)**.

7. Some Examples of Lunar Pseudo-Volcanic Eruptions

In this section, some features of the lunar volcanoes Alphonsus, Haldane-Tasso, Compton, and Oppenheimer will be considered. Magmatic deposits in these craters are highlighted above in **Figure 12** with color triangles.

The topography of Alphonsus and the spatial distribution of pyroclastic volcanic depositions are shown in **Figure 13(a)**. Additionally, in the area adjacent to Alphonsus crater, the cross-section of Kaguya topographies along white dashed lines was studied, see **Figure 13(b)**. As shown in **Figure 13(b)**, the lunar crater Alphonsus has a diameter of ~117.2 km. The walls of the crater are vertical, and the depth of the crater is 1400 - 2000 m. In the center of Alphonsus crater there is a peak of steaming-pipe, whose height is about ~500 m. The center of crater and circular rock dump (blowout ring) are highlighted in **Figure 13(b)** by vertical dash lines. The blowout system of Alphonsus has a single ring. Pyroclastic

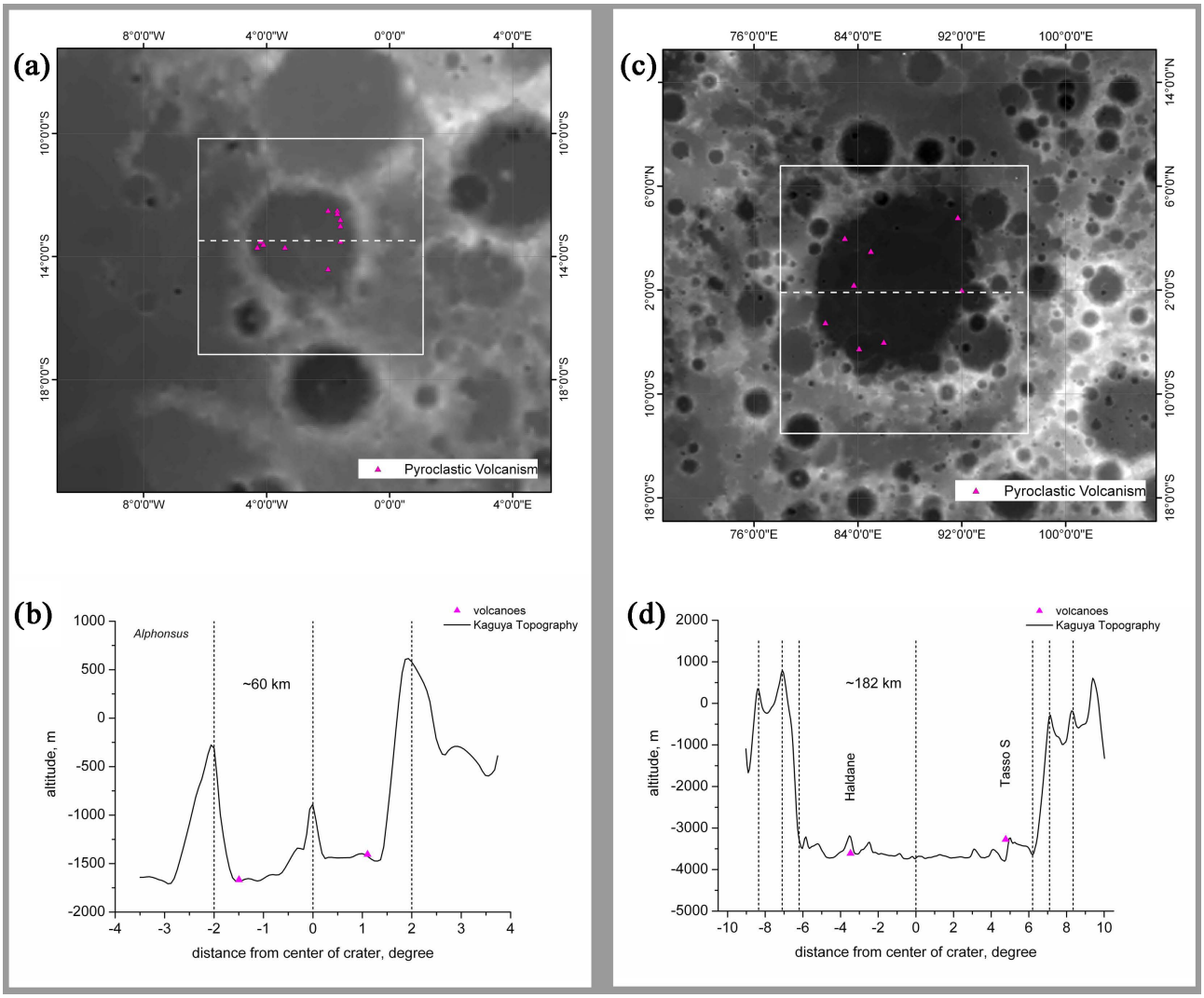

Figure 13. The craters Alphonsus and Haldane-Tasso with the spatial distribution of pyroclastic volcanic depositions are shown in (a) and (c). Cross-sections of the topography of Kaguya in the area of the craters Alphonsus and Haldane-Tasso (white dashed lines) are shown in (b) and (d). The crater Alphonsus has a peak in the center, while the Haldane-Tasso crater system has a flat basin in the center of the crater.

volcanic depositions (margin triangles) are located along the blowout ring at the bottom of the crater. Some information about Alphonsus could be found in [73] [74] [75].

In contrast to Alphonsus, we presented the Haldane-Tasso crater system in **Figure 13(c)** and **Figure 13(d)**. This system has a flat basin in the center of the crater and a two-ring blowout system; please see the vertical dash lines in **Figure 13(d)**. Also, as for Alphonsus, the walls of the crater are high and vertical. Pyroclastic volcanic depositions are located on the bottom of cater nearby crater's walls. The height of the crater wall is in the range of 3000 - 4000 m. The diameter of the crater is ~367 km.

Below we give a couple more examples of different types of pseudo-volcanic processes. The orography of Compton and Oppenheimer craters with the spatial

distribution of pyroclastic volcanic depositions is shown in Figure 14(a) and Figure 14(c). The cross-sections of these craters along the white dashed lines, which are shown in Figure 13(a) and Figure 13(c), are drawn in Figure 14(b) and Figure 14(d), respectively. The Compton crater has a large steaming-pipe peak in the center, while the Oppenheimer crater has a hollow in the center of the crater. Thus, Compton crater is a fuming behavior pseudo volcano, which has probably been fuming for a long time, while Oppenheimer looks like an explosive lunar pseudo volcano, in which the collapsed pingo is stuck in the central streaming pipe. In both of these studied cases, pyroclastic volcanic depositions are located near the crater walls and are the result of the collapse of heavy pingo cupolas. Note that the Compton-Belkovich volcanic complex has been well investigated, so a detailed description of ash flows can be found, e.g. in [76] [77] [78] [79].

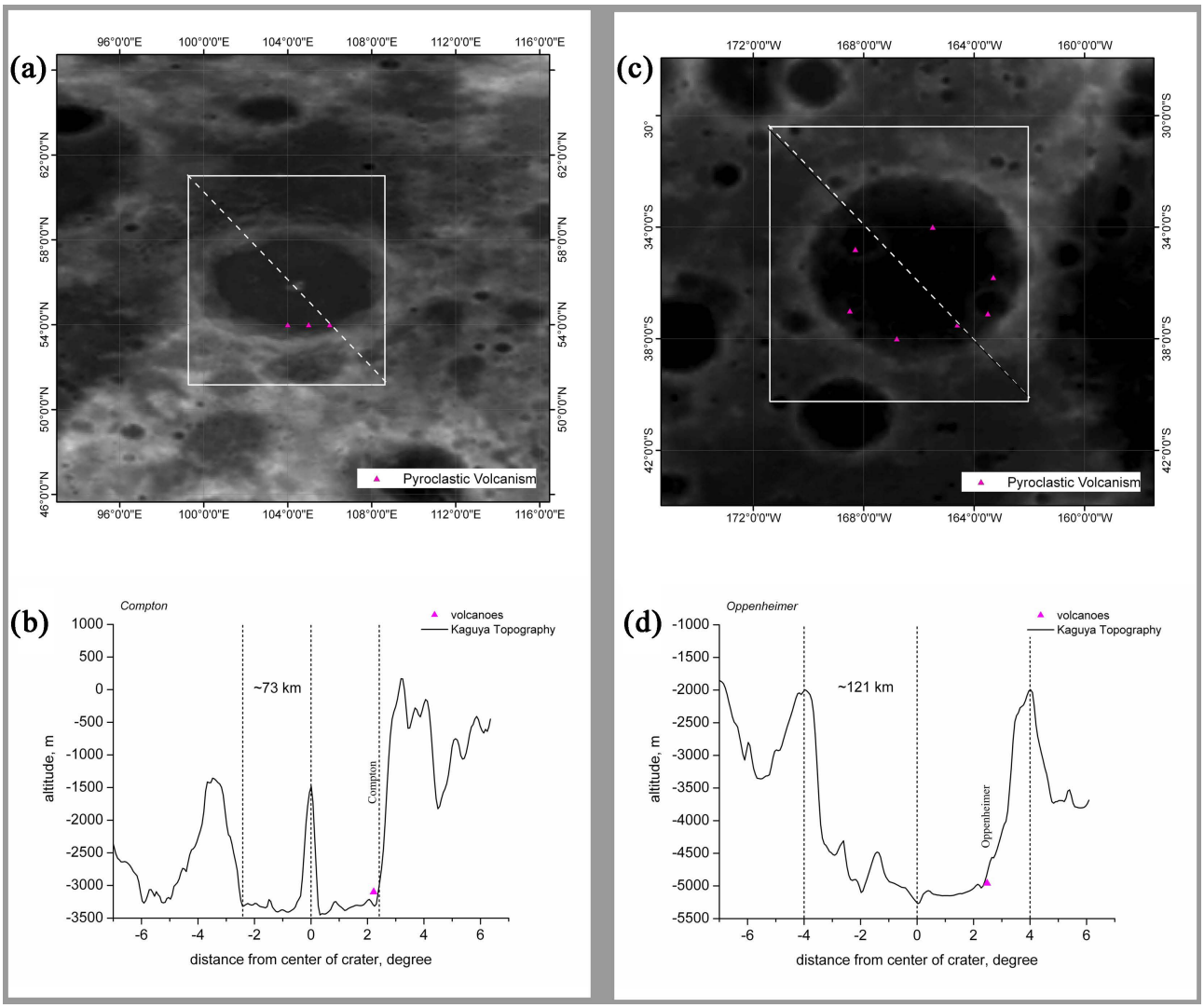

Figure 14. The Compton and Oppenheimer craters with the spatial distribution of pyroclastic volcanic depositions are shown in (a) and (c). Cross-sections of the Kaguya topographies in the area located near Compton and Oppenheimer craters (white dashed lines) are shown in (b) and (d). Compton crater has a peak in the center, while the Oppenheimer crater has a hollow in the center of the crater.

Summing up the above Sections 6 and 7, it should be stated that after the formation of the Moon, no additional volcanic activity was detected on its surface. Therefore, it is not possible to talk about additional saturation of the lunar surface with ores after the formation of the Moon, that is, during galactic storms.

8. Discussion

In this section, we get some remarks about ores, water, methane, diamonds, and life on the Moon. The basic equations for the transformation of the substance of a comet, which consisted mainly of carbon dioxide, are presented in the form of Equations 1 and 2.

$$CO_2 \rightarrow CO \rightarrow C \rightarrow \text{diamonds} \quad (1)$$

$$CO_2 + H \rightarrow \text{C-O-H} \rightarrow CH_4 + H_2O \rightarrow \ldots \rightarrow \text{OH-}CH_4\text{-OH} \rightarrow \ldots \rightarrow \text{life} \quad (2)$$

Due to the comet impact occurred in the southern hemisphere, below the southern edges of Africa and South America [14], Equation (1) is mainly implemented, leading to the formation of diamond deposits. Due to the time delay of detonation of the deepest nuclear layers of the protoplanet, Equation (2) is realized in the northern hemisphere. This explains the fact that the most of the gas and oil fields are concentrated in the northern hemisphere.

From other hand the Moon separated at the beginning of the separation process, so the first process described by Equation (1) dominates on the Moon with the formation of bubbles (pingos) and pseudo-volcanic craters after the destruction of these pingos. The formation of kimberlite pipes and diamonds is also expected, mainly on the farside of the Moon during the burning of the oldest protoplanet crust (**Figure 4(b)**). On the other hand, the amount of methane, oil and water on the Moon will be minimal. The absence of water explains the absence of living forms on the Moon, at least on the surface of the Moon. Note that the existence of forms of life in cavities filled with water and methane, under the lunar surface, is theoretically permissible; please see studies carrying out by Kadyshevich and Ostrovskii, see [80] and references authors about LOH theory. In this study it was investigated the role of methane hydrate, abbreviated as (OH-CH_4-OH) in Equation (2), in the life origin.

Further, on Moon according to [81] [82], the amount of methane (CH_4) and its isotope CD4 is minimal, so based on Equation 2, the probability of finding water (H_2O) is small. Also recall that in [67] [77] [79], and [83] [84] [85] it was written about the water content in the lunar magma.

In this study, ore formation is presented as a three-stage process, which included a comet impact, galaxy storms, and galaxy calm stage of ore formation. At different stages of the evolution of the planet and satellite, the process of ore formation differs greatly both in terms of the volume of ore formation and in their localization. The result of this study is summarized in **Table 1**.

The crisis in geology, geophysics and astrophysics arose due to the fact that the physical processes leading to the formation of ores, diamonds, oil, water and continents, as well as the formation of the Moon were carrying out by the methods

Table 1. The localization and qualitative comparison of the formation of ores, water, methane and diamonds at different stages of the evolution of the Moon-Earth system are presented.

Period	Creation	Earth		Moon	
		Southern hemisphere	North hemisphere	Nearside	Farside
comet impact	ores (intermediate and heavy elements)	oldest faults		more, scattering	less, in craters
	diamonds	more, large size	less, small size	none	probably
	water	none	yes	slightly	slightly
	methane and oil	none	yes	slightly	slightly
galaxy storm	ores (intermediate elements)	MORBs, LIPs		none	
galaxy calm	light elements, mainly sulphide	volcanic lavas and ashes		none	

of geochemistry and planetary astronomy. These methods could by no means give a correct description of the nuclear transformations occurring inside the protoplanet. Further, as noted above, each star is a natural reactor. Therefore, the situation in astrophysics is even more dramatic than in geophysics, since most astronomers and astrophysicists are not experts in nuclear sciences. Thus, a great deal of money and effort in geophysics and astrophysics has been spent trying to solve scientific problems with inappropriate methods and approaches. This is regrettable.

9. Conclusions

In this work, the theory of ore formation on the Earth and on the Moon is being developed. This theory of the spatial distribution of ores on the Earth and Moon is based on the Elemental Buoyancy Theory (EBT), developed by the author earlier. The main results are as follows:

r1. It is shown that ore deposits on the Earth and the Moon were mainly formed simultaneously, as a result of the release of intermediate and heavy elements from the deep layers of the protoplanet Earth. The formation of ore deposits occurred simultaneously with the formation of continents, with ores stuck in the oldest terrestrial geological faults.

r2. The time of formation of the lunar and terrestrial ores corresponds to the boundary between the Tonian and Cryogenic geological periods, *i.e.* ~750 Ma, taking into account the accuracy of dating of these periods.

r3. It was shown that the ore formation is a three-stage process during a collision with a comet (Figure 1(a)), galaxy storms (Figure 1(b)), and galaxy calm (Figure 1(c)). At different stages of the evolution of the planet and satellite, the process of ore formation differs greatly both in terms of the volume of ore formation and in their localization.

r4. Due to the impact of a comet in the southern hemisphere, more diamond deposits have been discovered in this hemisphere than in the northern hemisphere. However, in the southern hemisphere, the size and quality of diamonds

are higher. At the same time, the nuclear synthesis of water and various hydrocarbons took place in the northern hemisphere under terrestrial lithospheric plates. On Earth, life also originated in the northern hemisphere.

r5. On the near and far sides of the Moon, the processes of ore formations are different. The far side of the Moon is a single piece of the protoplanet's crust. Therefore, the lunar ores on this side could have been formed mainly due to the overflow of igneous rocks over the edge of the lunar continent, that is, they can be distributed in the boundary zone or in local zones of burning of the lunar lithospheric plate, *i.e.* at the bottom of pseudo-volcanic craters (pingos). On the visible side of the Moon, due to the rapid cooling of ores, they could form in the constriction region of a drop-stream separation. At the same time, the heavier elements lifted by the explosion from the deeper zones of the protoplanet are scattered less and concentrated in the central part on the visible side of the Moon. Due to the fact that the Moon separated at the first stage, the amount of water and methane on it is limited, but diamond synthesis is expected mainly on the farside of the satellite.

r6. The enrichment of the surface of the Earth is possible due to volcanic and seismic activities in the LIPs and MORBs areas during galaxy storms. It is assumed that sedimentary rocks on Earth could have been enriched with intermediate elements of the periodic system due to the disruption of vertical stratification at the galaxy storms.

r7. During the entire period after the formation of the Moon, no additional volcanic activity was detected on its surface. Therefore, it is not possible to talk about additional saturation of the lunar surface with ores after Moon formation, in particular, during galactic storms.

While this paper is primarily theoretical, it offers a fresh perspective on the creation of the Earth and Moon that may shed light on the origins of the universe. By delving into the genesis of our planet and its satellite, we may gain a better understanding of the wider cosmic picture. Additionally, these insights could prove useful in future lunar exploration and resource exploitation efforts.

Conflicts of Interest

The author declares no conflicts of interest regarding the publication of this paper.

References

[1] Kuroda, P. (1960) Nuclear Fission in the Early History of the Earth. *Nature*, **187**, 36-38. https://doi.org/10.1038/187036a0

[2] Hollenbach, D.F. and Herndon, J.M. (2001) Deep-Earth Reactor: Nuclear Fission, Helium, and the Geomagnetic Field. *Proceedings of the National Academy of Sciences of the United States of America* (*PNAS*), **98**, 11085-11090. https://doi.org/10.1073/pnas.201393998

[3] Herndon, J.M. (2003) Nuclear Georeactor Origin of Oceanic Basalt 3He/4He, Evidence, and Implications. *Proceedings of the National Academy of Sciences of the*

United States of America (*PNAS*), **100**, 3047-3050.
https://doi.org/10.1073/pnas.0437778100

[4] Herndon, J.M. (2014) Terracentric Nuclear Fission Georeactor: Background, Basis, Feasibility, Structure, Evidence and Geophysical Implications. *Current Science*, **106**, 528-541.

[5] Herndon, J.M. (2011) Corruption of Science in America. *The Dot Connector Magazine*, **2**, 25-32. http://nuclearplanet.com/corruption.pdf

[6] Fogli, G., Lisi, E., Palazzo, A. and Rotunno, A. (2005) KamLAND Neutrino Spectra in Energy and Time: Indications for Reactor Power Variations and Constraints on the Georeactor. *Physics Letters B*, **623**, 80-92.
https://doi.org/10.1016/j.physletb.2005.07.064

[7] Dye, S., Guillian, E., Learned, J., Maricic, J., Matsuno, S., Pakvasa, S., Varner, G. and Wilcox, M. (2006) Earth Radioactivity Measurements with a Deep Ocean Antineutrino Observatory. *Earth, Moon, and Planets*, **99**, 241-252.
https://doi.org/10.1007/s11038-006-9129-z

[8] Dye, S.T. (2009) Neutrino Mixing Discriminates Geo-Reactor Models. *Physics Letters B*, **679**, 15-18. https://doi.org/10.1016/j.physletb.2009.07.010

[9] Fogli, G.L., Lisi, E., Palazzo, A. and Rotunno, A.M. (2010) Combined Analysis of KamLAND and Borexino Neutrino Signals from Th and U Decays in the Earth's Interior. *Physical Review D*, **82**, Article ID: 093006.
https://doi.org/10.1103/PhysRevD.82.093006

[10] Gando, A. and KamLAND Collaboration (2013) Reactor On-Off Antineutrino Measurement with KamLAND. *Physical Review D*, **88**, Article ID: 033001.
https://doi.org/10.1103/PhysRevD.88.033001

[11] Agostini, M. and Borexino Collaboration (2015) Spectroscopy of Geoneutrinos from 2056 Days of Borexino Data. *Physical Review D*, **92**, Article ID: 031101.
https://doi.org/10.1103/PhysRevD.92.031101

[12] Roncin, R. and Borexino Collaboration (2016) Geo-Neutrino Results with Borexino. *Journal of Physics: Conference Series*, **675**, Article ID: 012029.

[13] Ludhova, L. and Zavatarelli, S. (2013) Studying the Earth with Geoneutrinos. *Advances in High Energy Physics*, **2013**, Article ID: 425693.
https://doi.org/10.1155/2013/425693

[14] Safronov, A.N. (2016) The Basic Principles of Creation of Habitable Planets around Stars in the Milky Way Galaxy. *International Journal of Astronomy and Astrophysics*, **6**, 512-554. https://doi.org/10.4236/ijaa.2016.64039

[15] Safronov, A.N. (2020) A New View of the Mass Extinctions and the Worldwide Floods. *International Journal of Geosciences*, **11**, 251-287.
https://doi.org/10.4236/ijg.2020.114014

[16] Safronov, A.N. (2022) New Theory of Effusive and Explosive Volcanic Eruptions. *International Journal of Geosciences*, **13**, 115-137.
https://doi.org/10.4236/ijg.2022.132007

[17] Safronov, A.N. (2022) Astronomical Triggers as a Cause of Strong Earthquakes. *International Journal of Geosciences*, **13**, 793-829.
https://doi.org/10.4236/ijg.2022.139040

[18] Safronov, A.N. (2023) Life Origin in the Milky Way Galaxy: I. The Stellar Nucleogenesis of Elements Necessary for the Life Origin.
https://www.preprints.org/manuscript/202305.0202/v1
https://doi.org/10.20944/preprints202305.0202.v1

[19] Safronov, A.N. (2023) Life Origin in the Milky Way Galaxy: II. Scanning for Habitable Stellar Systems on Behalf of Future Space Missions.
https://www.preprints.org/manuscript/202305.0005/v1
https://doi.org/10.20944/preprints202305.0005.v1

[20] Safronov, A.N. (2023) Life Origin in the Milky Way Galaxy: III. Spatial Distribution of Overheated Stars in the Solar Neighborhood.
https://www.preprints.org/manuscript/202305.0006/v1
https://doi.org/10.20944/preprints202305.0006.v1

[21] Prettyman, T.H., Hagerty, J.J., Elphic, R.C., Feldman, W.C., Lawrence, D.J., McKinney, G.W. and Vaniman, D.T. (2006) Elemental Composition of the Lunar Surface: Analysis of Gamma Ray Spectroscopy Data from Lunar Prospector. *Journal of Geophysical Research*, *Planet*, **111**, E12007.
https://doi.org/10.1029/2005JE002656

[22] Dataset (2010) Global GIS Lunar.
https://pdsimage2.wr.usgs.gov/pub/pigpen/moon/Global_GIS_Lunar/LunarGISDVD_v08.zip

[23] Gaddis, L., Rosanova, C., Hare, T., Hawke, B.R., Coombs, C. and Robinson, M.S. (1998) Small Lunar Pyroclastic Deposits: A New Global Perspective. *Lunar Planetary Science*, **29**, 1807-1808.

[24] Gaddis, L.R., Staid, M.I., Tyburczy, J.A., Hawke, B.R. and Petro, N.E. (2003) Compositional Analyses of Lunar Pyroclastic Deposits. *Icarus*, **161**, 262-280.
https://doi.org/10.1016/S0019-1035(02)00036-2

[25] Description of GIS System (2021) ArcInfo, ERSI.

[26] Brush, S. (1988) A History of Modern Selenogony: Theoretical Origins of the Moon, from Capture to Crash 1955-1984. *Space Science Reviews*, **47**, 211-273.
https://doi.org/10.1007/BF00243556

[27] Darwin, G.H. (1879) On the Bodily Tides of Viscous and Semi-Elastic Spheroids, and on the Ocean Tides upon a Yielding Nucleus. *Philosophical Transactions of the Royal Society of London*, **170**, 1-35. https://doi.org/10.1098/rstl.1879.0061

[28] Wise, D.U. (1969) Origin of the Moon from the Earth: Some New Mechanisms and Comparisons. *Journal of Geophysical Research*: *Planets*, **74**, 6034-6045.
https://doi.org/10.1029/JB074i025p06034

[29] Ringwood, A.E. (1986) Composition and Origin of the Moon. In: Hartmann, W.K., Ed., *Origin of the Moon*, Lunar and Planetary Institute, Houston, 673-698.

[30] Safronov, V.S. (1991) Kuiper Prize Lecture: Some Problems in the Formation of the Planets. *Icarus*, **94**, 260-271. https://doi.org/10.1016/0019-1035(91)90226-J

[31] Safronov, V. and Ruskol, E. (1994) Formation and Evolution of Planets. *Astrophysics and Space Science*, **212**, 13-22. https://doi.org/10.1007/BF00984504

[32] Benz, W., Slattery, W.L. and Cameron, A.G.W. (1986) The Origin of the Moon and the Single-Impact Hypothesis I. *Icarus*, **66**, 515-535.
https://doi.org/10.1016/0019-1035(86)90088-6

[33] Benz, W., Slattery, W.L. and Cameron, A.G.W. (1987) The Origin of the Moon and the Single-Impact Hypothesis II. *Icarus*, **71**, 30-45.
https://doi.org/10.1016/0019-1035(87)90160-6

[34] Benz, W., Cameron, A.G.W. and Melosh, H.J. (1989) The Origin of the Moon and the Single-Impact Hypothesis III. *Icarus*, **81**, 113-131.
https://doi.org/10.1016/0019-1035(89)90129-2

[35] Cameron, A.G.W. and Benz, W. (1991) The Origin of the Moon and the Single Im-

pact Hypothesis IV. *Icarus*, **92**, 204-216. https://doi.org/10.1016/0019-1035(91)90046-V

[36] Cameron, A.G.W. (1997) The Origin of the Moon and the Single Impact Hypothesis V. *Icarus*, **126**, 126-137. https://doi.org/10.1006/icar.1996.5642

[37] Canup, R.M. (2012) Forming a Moon with an Earth-Like Composition via a Giant Impact. *Science*, **338**, 1052-1055. https://doi.org/10.1126/science.1226073

[38] Canup, R.M. (2013) Lunar Conspiracies. *Nature*, **504**, 27-29. https://doi.org/10.1038/504027a

[39] Canup, R.M. (2014) Lunar-Forming Impacts: Processes and Alternatives. *Philosophical Transactions of the Royal Society A*: *Mathematical*, *Physical and Engineering Sciences*, **372**, Article ID: 20130175. https://doi.org/10.1098/rsta.2013.0175

[40] Canup, R.M., Visscher, C., Salmon, J. and Fegley Jr., B. (2015) Lunar Volatile Depletion Due to Incomplete Accretion within an Impact-Generated Disk. *Nature Geoscience*, **8**, 918-921. https://doi.org/10.1038/ngeo2574

[41] Clayton, R.N. and Mayeda, T.K. (1996) Oxygen Isotopic Studies of Achondrites. *Geochimica et Cosmochimica Acta*, **60**, 1999-2017. https://doi.org/10.1016/0016-7037(96)00074-9

[42] Wiechert, U., Halliday, A.N., Lee, D.C., Snyder, G.A., Taylor, L.A. and Rumble, D. (2001) Oxygen Isotopes and the Moon-Forming Giant Impact. *Science*, **294**, 345-348. https://doi.org/10.1126/science.1063037

[43] Shukolyukov, A. and Lugmair, G.W. (2000) On the ^{53}Mn Heterogeneity in the Early Solar System. *Space Science Reviews*, **92**, 225-236. https://doi.org/10.1007/978-94-011-4146-8_15

[44] Trinquier, A., Birck, J.L., Allegre, C.J., Gopel, C. and Ulfbeck, D. (2008) ^{53}Mn-^{53}Cr Systematics of the Early Solar System Revisited. *Geochimica et Cosmochimica Acta*, **72**, 5146-5163. https://doi.org/10.1016/j.gca.2008.03.023

[45] Leya, I., Schonbachler, M., Wiechert, U., Krahenbuhl, U. and Halliday, A.N. (2008) Titanium Isotopes and the Radial Heterogeneity of the Solar System. *Earth and Planetary Science Letters*, **266**, 233-244. https://doi.org/10.1016/j.epsl.2007.10.017

[46] Zhang, J., Dauphas, N., Davis, A.M., Leya, I. and Fedkin, A. (2012) The Proto-Earth as a Significant Source of Lunar Material. *Nature Geoscience*, **5**, 251-255. https://doi.org/10.1038/ngeo1429

[47] Georg, R.B., Halliday, A.N., Schauble, E.A. and Reynolds, B.C. (2007) Silicon in the Earth's Core. *Nature*, **447**, 1102-1106. https://doi.org/10.1038/nature05927

[48] Fitoussi, C. and Bourdon, B. (2012) Silicon Isotope Evidence against an Enstatite Chondrite Earth. *Science*, **335**, 1477-1480. https://doi.org/10.1126/science.1219509

[49] Voronin, D.V. (2011) Computer Modeling of Planet Partial Fragmentation. *WSEAS Transactions on Fluid Mechanics*, **1**, 32-50.

[50] de Meijer, R.J., Anisichkin, V.F. and van Westrenen, W. (2013) Forming the Moon from Terrestrial Silicate-Rich Material. *Chemical Geology*, **345**, 40-49. https://doi.org/10.1016/j.chemgeo.2012.12.015

[51] Rufu, R., Aharonson, O. and Perets, H.B. (2017) A Multiple-Impact Origin for the Moon. *Nature Geoscience*, **10**, 89-94. https://doi.org/10.1038/ngeo2866

[52] Deng, H., Ballmer, M.D., Reinhardt, C., Meier, M.M.M., Mayer, L., Stadel, J. and Benitez, F. (2019) Primordial Earth Mantle Heterogeneity Caused by the Moon-Forming Giant Impact? *The Astrophysical Journal*, **887**, 211. https://doi.org/10.3847/1538-4357/ab50b9

[53] Righter, K. (2019) Volatile Element Depletion of the Moon—The Roles of Precursors, Post-Impact Disk Dynamics, and Core Formation. *Science Advances*, **5**, eaau7658. https://doi.org/10.1126/sciadv.aau7658

[54] Rufu, R. and Canup, R.M. (2020) Tidal Evolution of the Evection Resonance/Quasia-Resonance and the Angular Momentum of the Earth-Moon System. *Journal of Geophysical Research*: *Planets*, **125**, e2019JE006312. https://doi.org/10.1029/2019JE006312

[55] Wissing, R. and Hobbs, D. (2020) A New Equation of State Applied to Planetary Impacts. 2. Lunar-Forming Impact Simulations with a Primordial Magma Ocean. *Astronomy & Astrophysics*, **643**, A40. https://doi.org/10.1051/0004-6361/201936227

[56] Kegerreis, J.A., Ruiz-Bonilla, S., Eke, V.R., Massey, R.J., Sandnes, T.D. and Teodoro, L.F.A. (2022) Immediate Origin of the Moon as a Post-Impact Satellite. *The Astrophysical Journal Letters*, **937**, L40. https://doi.org/10.3847/2041-8213/ac8d96

[57] Rufu, R., Salmon, J., Pahlevan, K., Visscher, C., Nakajima, M. and Righter, K. (2021) The Origin of the Earth-Moon System as Revealed by the Moon. Planetary Science and Astrobiology Decadal Survey Science, Whitepaper #238. https://doi.org/10.3847/25c2cfeb.6e7d4ab6

[58] Canup, R.M., Righter, K., Dauphas, N., Pahlevan, K., Ćuk, M., Lock, S.J., Stewart, S.T., Salmon, J., Rufu, R., Nakajima, M. and Magna, T. (2021) Origin of the Moon. https://arxiv.org/ftp/arxiv/papers/2103/2103.02045.pdf

[59] Burbidge, E.M., Burbidge, G.R., Fowler, W.A. and Hoyle, F. (1957) Synthesis of the Elements in Stars. *Reviews of Modern Physics*, **29**, 547-650. https://doi.org/10.1103/RevModPhys.29.547

[60] Kobayashi, C., Karakas, A.I. and Lugaro, M. (2020) The Origin of Elements from Carbon to Uranium. *The Astrophysical Journal*, **900**, 179. https://doi.org/10.3847/1538-4357/abae65

[61] Cohen, K.M., Finney, S.M., Gibbard, P.L. and Fan, J.-X. (2013) The ICS International Chronostratigraphic Chart. *Episodes*, **36**, 199-204. https://www.episodes.org https://doi.org/10.18814/epiiugs/2013/v36i3/002

[62] Cohen, K.M., Harper, D.A.T. and Gibbard, P.L. (2020) ICS International Chronostratigraphic Chart 2020/03. International Commission on Stratigraphy, IUGS. https://stratigraphy.org/ICSchart/ChronostratChart2022-02.pdf

[63] Burr, D.M., Tanaka, K.L. and Yoshikawa, K. (2009) Pingos on Earth and Mars. *Planetary and Space Science*, **57**, 541-555. https://doi.org/10.1016/j.pss.2008.11.003

[64] Colin, M.D. and McEwen, A.S. (2010) An Assessment of Evidence for Pingos on Mars Using HiRISE. *Icarus*, **205**, 244-258. https://doi.org/10.1016/j.icarus.2009.02.020

[65] Soare, R.J., Conway, S.J., Pearce, G.D., Dohm, J.M. and Grindrod, P.M. (2013) Possible Crater-Based Pingos, Paleolakes and Periglacial Landscapes at the High Latitudes of Utopia Planitia, Mars. *Icarus*, **225**, 971-981. https://doi.org/10.1016/j.icarus.2012.08.041

[66] Wetzel, D.T., Hauri, E.H., Saal, A.E. and Rutherford, M.J. (2014) Dissolved Carbon Content of the Lunar Volcanic Glass Beads and Melt Inclusions: Carbon from the Lunar Interior. 45*th Lunar and Planetary Science Conference*, Houston, 17-21 March 2014, 2238.

[67] Wetzel, D.T., Hauri, E.H., Saal, A.E. and Rutherford, M.J. (2015) Carbon Content and Degassing History of the Lunar Volcanic Glasses. *Nature Geoscience*, **8**, 755-758. https://doi.org/10.1038/ngeo2511

[68] Needham, D.H. and Kring, D.A. (2017) Lunar Volcanism Produced a Transient Atmosphere around the Ancient Moon. *Earth and Planetary Science Letters*, **478**, 175-178. https://doi.org/10.1016/j.epsl.2017.09.002

[69] Yokota, S., Terada, K., Saito, Y., Kato, D., Asamura, K., Nishino, M.N., Shimizu, H., Takahashi, F., Shibuya, H., Matsushima, M. and Tsunakawa, H. (2020) KAGUYA Observation of Global Emissions of Indigenous Carbon Ions from the Moon. *Science Advances*, **6**, eaba1050. https://doi.org/10.1126/sciadv.aba1050

[70] Colaprete, A., Schultz, P., Heldmann, J., Wooden, D., Shirley, M.H., Ennico, K., Hermalyn, B., Marshall, W., Ricco, A., Elphic, R.C., Goldstein, D.B., Summy, D., Bart, G., Asphaug, E., Korycansky, D., Landis, D. and Sollit, L. (2010) Detection of Water in the LCROSS Ejecta Plume. *Science*, **330**, 463-468. https://doi.org/10.1126/science.1186986

[71] Schorghofer, N., Williams, J.-P., Martinez-Camacho, J., Paige, D.A. and Siegler, M.A. (2021) Carbon Dioxide Cold Traps on the Moon. *Geophysical Research Letters*, **48**, e2021GL095533. https://doi.org/10.1029/2021GL095533

[72] Araki, H., Tazawa, S., Noda, H., Ishihara, Y., Goossens, S., Sasaki, S., Kawano, N., Kamiya, I., Otake, H., Oberst, J. and Shum, C. (2009) Lunar Global Shape and Polar Topography Derived from Kaguya-LALT Laser Altimetry. *Science*, **323**, 897-900. https://doi.org/10.1126/science.1164146

[73] Gaddis, L.R., Klem, S., Gustafson, J.O., Hawke, B.R. and Giguere, T.A. (2011) Alphonsus Dark-Halo Craters: Identification of Additional Volcanic Vents. 42*th Lunar and Planetary Science Conference*, The Woodlands, 7-11 March 2011, 2691.

[74] Skinner, J., J. A., Gaddis, L.R., Keszthelyi, L., Hare, T.M., Howington-Kraus, E. and Rosiek, M. (2005) Alphonsus-Type Dark-Halo Craters—Morphometry and Volume Reassessments and Implications for Eruptive Style. 36*th Lunar and Planetary Science Conference*, League City, 14-18 March 2005, 2344.

[75] Head, J.W. and Wilson, L. (2016) Generation, Ascent and Eruption of Magma on the Moon: New Insights into Source Depths, Magma Supply, Intrusions and Effusive/Explosive Eruptions (Part 2: Predicted Emplacement Processes and Observations). *Icarus*, **283**, 176-223. https://doi.org/10.1016/j.icarus.2016.05.031

[76] Jolliff, B.L., Wiseman, S.A., Lawrence, S.J., Tran, T.N., Robinson, M.S., Sato, H., Hawke, B.R., Scholten, F., Oberst, J., Hiesinger, H., van der Bogert, C.H., Greenhagen, B.T., Glotch, T.D. and Paige, D.A. (2011) Non-Mare Silicic Volcanism on the Lunar Farside at Compton-Belkovich. *Nature Geoscience*, **4**, 566-571. https://doi.org/10.1038/ngeo1212

[77] Petro, N.E., Isaacson, P.J., Pieters, C.M., Jolliff, B.L., Carter, L.M. and Klima, R.L. (2013) Presence of OH/H20 Associated with the Lunar Compton-Belkovich Volcanic Complex Identified by the Moon Mineralogy Mapper (M3). 44*th Lunar and Planetary Science Conference*, The Woodlands, 18-22 March 2013, 2688.

[78] Chauhan, M., Bhattacharya, S., Saran, S., Chauhan, P. and Dagar, A. (2015) Compton-Belkovich Volcanic Complex (CBVC): An Ash Flow Caldera on the Moon. *Icarus*, **253**, 115-129. https://doi.org/10.1016/j.icarus.2015.02.024

[79] Wilson, L. and Head, J.W. (2016) Explosive Volcanism Associated with the Silicic Compton-Belkovich Volcanic Complex: Implications for Magma Water Content. 47*th Lunar and Planetary Science Conference*, The Woodlands, 21-25 March 2016, 1564.

[80] Kadyshevich, E.A. and Ostrovskii, V.E. (2023) From Minerals to Simplest Living Matter: Life Origination Hydrate Theory. *Acta Biotheoretica*, **71**, Article No. 13. https://doi.org/10.1007/s10441-023-09463-9

[81] Cadogan, P.H., Eglinton, G., Maxwell, J.R. and Pillinger, C.T. (1971) Carbon Che-

mistry of the Lunar Surface. *Nature*, **231**, 29-31. https://doi.org/10.1038/231029a0

[82] Jull, A.J.T., Eglinton, G., Pillinger, C.T., Biggar, G.M. and Batts, B.D. (1976) The Identity of Lunar Hydrolysable Carbon. *Nature*, **262**, 566-567. https://doi.org/10.1038/262566a0

[83] Saal, A.E., Hauri, E.H., Cascio, M.L., Van Orman, J.A., Rutherford, M.C. and Cooper, R.F. (2008) Volatile Content of Lunar Volcanic Glasses and the Presence of Water in the Moon's Interior. *Nature*, **454**, 192-195. https://doi.org/10.1038/nature07047

[84] Hauri, E.H., Weinreich, T., Saal, A.E., Rutherford, M.C. and Van Orman, J.A. (2011) High Pre-Eruptive Water Contents Preserved in Lunar Melt Inclusions. *Science*, **333**, 213-215. https://doi.org/10.1126/science.1204626

[85] Hauri, E.H., Saal, A.E., Rutherford, M.J. and Van Orman, J.A. (2015) Water in the Moon's Interior: Truth and Consequences. *Earth and Planetary Science Letters*, **409**, 252-264. https://doi.org/10.1016/j.epsl.2014.10.053